

# Simulation of Deformation and Flow in Fractured, Poroelastic Materials

KATJA K. HANOWSKI\* and OLIVER SANDER†

Institut für Numerische Mathematik, TU Dresden, Germany

November 27, 2024

We introduce a coupled system of partial differential equations for the modeling of the fluid–fluid and fluid–solid interaction in a poroelastic material with a single static fracture. The fluid flow in the fracture is modeled by a lower-dimensional Darcy equation, which interacts with the surrounding rock matrix and the fluid it contains. We explicitly allow the fracture to end within the domain, and the fracture width is an unknown of the problem. The resulting weak problem is nonlinear, elliptic and symmetric, and can be given the structure of a fixed-point problem. We show that the coupled fluid–fluid problem has a solution in a specially crafted Sobolev space, even though the fracture width cannot be bounded away from zero near the crack tip.

For numerical simulations, we combine XFEM discretizations for the rock matrix deformation and pore pressure with a standard lower-dimensional finite element method for the fracture flow problem. The resulting coupled discrete system consists of linear subdomain problems coupled by nonlinear coupling conditions. We solve the coupled system with a substructuring solver and observe very fast convergence. We also observe optimal mesh dependence of the discretization errors even in the presence of crack tips.

## 1 Introduction

Coupled fluid–solid interaction processes in fractured porous media play an important role in engineering applications such as the design and construction of geothermal power plants, the risk assessment of waste deposits, and the production of crude oil and gas. Numerical simulation of such processes is an important tool for such applications. Furthermore it can help researchers in geosciences to gain a better understanding of intricate subsurface processes. Simulation remains challenging due to the number of physical processes involved, the nonlinear coupling, the complex geometries, and the heterogeneous nature of fractured porous rock. In particular, such systems combine hydrological processes such as fluid flow in the porous matrix and in the fracture network with mechanical effects: the deformation of the medium under fluid pressure and external loads.

In this work we focus on the nonlinear coupling between hydrology and mechanics. We consider a low-porosity medium containing a single large-scale fracture, which is filled with a porous medium without mechanical stiffness. Also, we assume that the fracture length scale is much larger than the fracture width. The pore space of the matrix and the fracture are both assumed to be fully saturated with a fluid. The mechanical and hydrological equilibrium state of the system is then governed by four coupling processes:

---

\*Katja.Hanowski@tu-dresden.de

†Oliver.Sander@tu-dresden.de

1. Fluid–fluid coupling: The fluid may diffuse from the fracture into the surrounding medium and vice versa.
2. Fluid–solid coupling: The fluid in the fracture exerts a normal force onto the fracture boundaries, which induces a deformation of the rock matrix.
3. Solid–fluid coupling: The deforming rock matrix changes the fracture domain, which affects the permeability in the fracture.
4. Poroelasticity: Fluid pressure in the rock matrix influences the matrix stiffness.

The third list item is the main challenge. The crack width enters the fracture flow equation as the inverse permeability, which renders the overall system nonlinear. The problem becomes even more challenging if the crack ends within the domain, which we explicitly allow. In such a case singularities appear near the crack tip both in the mechanical stresses and in the matrix fluid flow field. These singularities need to be captured by special singularity functions as part of the XFEM discretization. Optimal convergence of the discretization errors can only be observed if these functions are selected correctly. Furthermore, the crack width necessarily tapers off near the crack tip, and therefore cannot be bounded away from zero on the entire domain. Our proof of the existence of solutions to the coupled bulk–fracture fluid problem constructs particular weighted Sobolev spaces to deal with this degeneracy.

Elasticity problems in fractured materials have been widely addressed in the literature during the last century. Analytical solutions have been derived for several special cases [18, 32], and the singular behavior of the solution near the fracture tip has been investigated [21]. Various numerical methods have been developed, often in connection with the modeling of fracture propagation [31, 1]. A breakthrough in the numerical modeling of crack growth processes was the eXtended Finite Element Method (XFEM) [26, 37, 29], which enriches the discrete function spaces by non/polynomial functions locally reproducing the discontinuity along the fracture and the stress singularities at the crack tip. XFEM overcomes the need to adapt the mesh to the discontinuities and singularities of the solution.

Concerning the modeling and simulation of fluid flow in fractured porous media, we only mention some recent articles related to the model presented in this paper. In [23] a coupled bulk–fracture fluid model is derived from standard single-phase Darcy equations where the fracture is represented as a lower-dimensional interface. It is assumed that the fracture and surrounding matrix are both filled with porous media with different material properties, and that the fracture separates the domain into two parts (i.e., there is no crack tip). Under the assumption that there exists a lower bound for the fracture aperture function, existence and uniqueness of solutions in standard Sobolev spaces is proved. The authors present a discrete domain decomposition formulation of the original transmission problem using Raviart–Thomas Finite Elements. In [2], the model from [23] is extended to consider fractures with crack tips. A cell-centered finite volume scheme is applied, and again, a grid adapted to the fracture is required for the discretization of the problem. Existence of a solution is proved by showing the convergence of the finite volume discretization to a function in a subspace of  $H_{\text{div}}$ .

Since the discretizations proposed in these two papers rely on a grid resolving the fracture, considering multiple interacting fractures or fracture networks becomes computationally expensive. A more flexible discretization is introduced in [7], where the authors use an extended  $(RT_0, P_0)$  Raviart–Thomas discretization of the mixed problem. The authors prove consistency, stability and convergence of the proposed numerical scheme in the case of a domain fully cut by a fracture. In [11], the ideas of the model from [23] are generalized to flows in fracture networks. The fluid pressure and velocity are allowed to jump at the fracture intersections, but the fluid interaction with the surrounding matrix is not considered. Again, an extended  $(RT_0, P_0)$  Raviart–Thomas discretization is applied to overcome the difficulty of matching grids at the intersections of multiple fractures. The model from [23] has been extended to two-phase flow [19, 13] and passive transport [14].

In contrast, literature addressing the coupling of flow and deformation in fractured media is scarce. In [34] the Biot theory is used to describe the matrix flow and deformation, and a reduced model is used for the flow in the network. Both models are coupled by a crack width function similar to our own

approach. The authors use lower-dimensional interface elements to represent the fracture, and an XFEM discretization to capture the discontinuity of the matrix displacement and the fracture intersections. Nonetheless, to enforce pressure continuity, they require that the interface is resolved by the bulk grid.

An alternative model for the coupling of deformation and flow uses the quasi-static Biot equation, a linearized model for slightly compressible single-phase fluids in the surrounding media, and a lubrication Darcy equation for modeling the flow in the fracture [17, 16]. Contrary to our own approach, this model includes changes in the porosity of the bulk medium, but requires continuity of the fluid pressure across the interface. Existence and uniqueness in weighted Sobolev spaces is proved for a simplified version of the fracture equation in which the fracture permeability is not influenced by the fracture width. The problem is discretized using finite elements on matching grids.

The article [15] considers a fully saturated porous medium with a semi-infinite fracture filled with a viscous fluid. The fluid flow inside the fracture is modeled using lubrication theory, and the fluid leak-off into the surrounding medium is modeled using Carter’s leak-off law. From known analytical solutions to the displacement of an elastic solid and lubrication theory, the authors derive asymptotic solutions for the fluid pressure inside the fracture, the fracture aperture function and the fracture opening under the assumption that the fracture propagates at a constant velocity.

Similarly, in [12], the surrounding medium is modeled as an impermeable, homogeneous, isotropic linear elastic solid. The fracture flow is modeled using a standard lubrication equation for incompressible flow between parallel plates. The equations are coupled by using the fluid pressure as Neumann boundary conditions on the fracture. The authors present an efficient XFEM based discretization using a hybrid explicit–implicit crack description. The main focus of the paper is the determination of the stress intensity factors without the influence of rigid body motions of the crack tip.

Finally, a phase-field approach to fracture propagation is presented in [24]. There, the variational approach to fracture propagation presented in [4] is extended to fully saturated porous media that contains a fracture. Contrary to [15], the fracture propagates only according to an energy minimization principle and may bifurcate. The numerical modeling of this problem remains a challenging and computationally expensive task (see also [35] and references therein).

The model and discretization proposed in this paper combine and generalize several of the previous approaches. In particular, we consider the interplay of *three* processes, viz. the fluid flow in the fracture and the bulk matrix, and the elastic deformation of the matrix. As the matrix deformation determines the fracture width, which in turn determines the fracture permeability, the resulting coupled three-field problem is nonlinear in an intricate way.

More specifically, we combine the model from [23] for the coupled fluid flow in the fracture and in the surrounding medium with the Biot equation for a linear poroelastic material. Both models are coupled by defining the crack width as the normal jump of the displacement and by prescribing the fracture fluid pressure as a normal force applied to the solid skeleton at the fracture fronts. We derive the weak formulation of the problem based on the primal form of the Darcy equations and the Biot equation. This weak form has a natural formulation as a fixed-point equation. The corresponding fixed-point iteration alternates between solution operators for the elastic deformation and for the coupled matrix–fracture flow problem. Both solution operators are linear, and the overall nonlinearity stems only from the nonlinear coupling of the deformation to the flow problem. Our model allows cracks to end within the bulk. While our prototype geometry in Figure 2 has only one crack tip, we can easily handle the case of a fracture with two tips, and of two-dimensional fractures in a three-dimensional bulk, where the crack tip is a one-dimensional line. The width function acts as degenerated and singular coefficient in the fluid equations.

As the main theoretical result we prove existence and uniqueness of weak solutions of the coupled matrix–fracture flow problem for fixed fracture width. This is reasonably straightforward if the fracture width is bounded from below away from zero (see [23, 2]). However, in our case the fracture width is an  $H_{00}^{\frac{1}{2}}$  function, and hence must go to zero near the crack tip. From the asymptotic expansion of the deformation field near the tip we deduce a general form of the fracture width function, which is used as weight in the definition of the solution spaces of the fluid problem. With the proper definition of these

spaces, we can prove existence and uniqueness of a solution of the fluid problem with fixed fracture width.

Unfortunately, proving existence of solutions of the overall fixed-point problem is not a matter of simply using an appropriate fixed-point theorem. Since the fracture width function enters the definition of the solution spaces for the fluid-problem, the fixed-point iteration actually operates on a sequence of iteration-dependent spaces. We leave this for future work.

We use an XFEM discretization both for the displacement and the fluid pressure. As a result we do not have any restriction on how the fracture is positioned relative to the bulk grid (unlike, e.g., [34, 17]). The major goal when designing a XFEM discretization is to make the space large enough to obtain optimal discretization error behavior for decreasing mesh size. This is particularly challenging in the presence of fracture tips, where singularities in the solution are to be expected. The optimal error behavior of correctly constructed XFEM discretizations for linear elasticity problems is well-known, and has been proved in [27]. Asymptotic analysis for the fluid problem in the bulk cannot be carried out straightforwardly, but known results can be used to conjecture the form of the crack tip singularity. Again, based on this result, the bulk solution of the pressure may admit a discontinuity across the fracture and a velocity singularity at the front. However, it is not clear at all whether the same still holds when combining such problems in a nonlinear fashion as we do here. While we have not attempted to prove rigorous bounds for the discretization errors of our XFEM approximation for the coupled fluid–fluid–elasticity problem, we observe optimal rates in numerical experiments. This leads us to conclude that the XFEM spaces used here are, in a certain sense, the correct ones.

The paper is organized as follows: In Chapter 2 we introduce the governing equations for the coupled processes. As a preparation for the weak formulation and the existence proofs, Chapter 3 introduces several weighted Sobolev spaces and shows some of their relevant properties. In Chapter 4, a weak formulation of the nonlinearly coupled problem is derived and we show existence and uniqueness of weak solutions of the fluid–fluid subproblem. In Chapter 5 we introduce an XFEM discretization of the resulting problem. Finally, Chapter 6 provides numerical examples showing that the discretization error behaves optimally.

## 2 The Coupled Deformation–Flow Model

We begin by stating the continuous model in its strong form. We do this in two steps: First we state the coupled equations for a system with a fully-dimensional fracture. In a separate step we then perform a dimension reduction of the fracture. This approach allows to better distinguish the features introduced by the coupling itself from those introduced by the dimension reduction.

### 2.1 Coupling Flow in a Full-Dimensional Fracture to a Poroelastic Bulk

Let  $\tilde{\Omega} \subset \mathbb{R}^d$  be a domain of dimension  $d = 2$  or  $d = 3$  with Lipschitz-boundary  $\tilde{\Gamma} := \partial\tilde{\Omega}$ . We assume that  $\tilde{\Omega}$  contains a fracture, which, in this first step, we model as a subdomain  $\Omega_f \subsetneq \tilde{\Omega}$  (Figure 1). Its complement  $\tilde{\Omega} \setminus \Omega_f$  will be denoted by  $\Omega_e$ .

#### 2.1.1 Flow Equations in the Fracture and the Matrix

We consider the matrix and the fracture to both consist of porous media, and to be both fully saturated with a single-phase incompressible fluid. These assumptions lead to the well-known Darcy equation

$$\operatorname{div} \mathbf{q} = f_F \quad \text{on } \tilde{\Omega}, \quad (1a)$$

$$\mathbf{q} = -\mathbb{K}\nabla p \quad \text{on } \tilde{\Omega}, \quad (1b)$$

where  $\mathbf{q}$  denotes the seepage velocity,  $p$  the pore pressure, and  $\mathbb{K} \in \mathbb{R}^{d \times d}$  the permeability tensor. In this formulation, the fracture  $\Omega_f$  appears as a region of  $\tilde{\Omega}$  where the permeability  $\mathbb{K}$  differs considerably

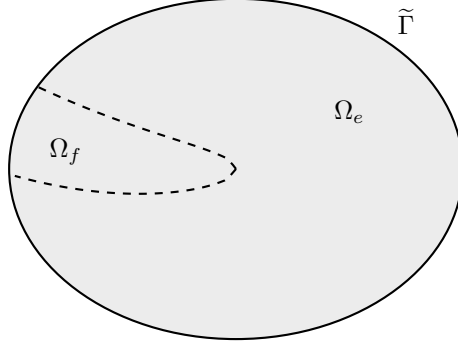


Figure 1: Domain  $\tilde{\Omega}$  with volume fracture  $\Omega_f$

from the rest. To prepare the inclusion into a coupled model, however, we formulate a substructuring problem. It is well known [30] that (1) is equivalent to solving the Darcy equation on the subdomains  $\Omega_e$  and  $\Omega_f$  separately, and imposing suitable coupling conditions. We therefore consider the system

$$\begin{aligned} \operatorname{div} \mathbf{q}^\Omega &= f_F^\Omega & \text{in } \Omega_e, \\ \mathbf{q}^\Omega &= -\mathbb{K}^\Omega \nabla p^\Omega & \text{in } \Omega_e, \end{aligned}$$

for the bulk and

$$\operatorname{div} \mathbf{q}^f = f^f \quad \text{in } \Omega_f, \quad (2a)$$

$$\mathbf{q}^f = -\mathbb{K}^f \nabla p^f \quad \text{in } \Omega_f, \quad (2b)$$

for the fracture. The appropriate coupling conditions for this are continuity of the pressure

$$p^\Omega = p^f \quad \text{on } \partial\Omega_e \cap \partial\Omega_f, \quad (3)$$

and continuity of the normal flux

$$\mathbf{q}^\Omega \cdot \nu_f = \mathbf{q}^f \cdot \nu_f \quad \text{on } \partial\Omega_e \cap \partial\Omega_f, \quad (4)$$

where  $\nu_f$  denotes the unit outer normal of  $\Omega_f$ . Well-posedness of this problem together with suitable boundary conditions is shown in [30].

### 2.1.2 Poroelastic Behavior of the Matrix

While the fracture and bulk are modeled as behaving qualitatively the same as far as hydrological processes are concerned, their mechanical behavior is considered to be different. While the bulk is described as a linear poroelastic material, we do not assign any stiffness to the fracture at all. Hence mechanically it behaves as if it was empty.

Let  $\mathbf{u} : \Omega_e \rightarrow \mathbb{R}^d$  be the displacement of the rock matrix. We make the small strain assumption, which allows to use the linearized strain

$$\mathbf{e}(\mathbf{u}) := \frac{1}{2} (\nabla \mathbf{u} + (\nabla \mathbf{u})^T)$$

and the St. Venant–Kirchhoff material law

$$\sigma(\mathbf{u}) = \lambda \operatorname{trace}(\mathbf{e}(\mathbf{u})) \mathbb{I} + 2\mu \mathbf{e}(\mathbf{u})$$

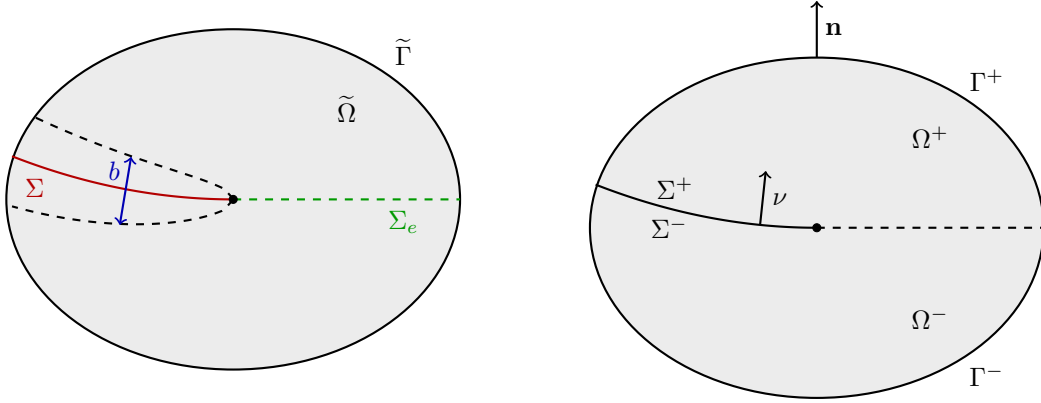


Figure 2: Replacing a thin fracture by a lower–dimensional approximation. Left: Fractured domain with fracture midsurface  $\Sigma$  and tangential extension  $\Sigma_e$ . Right: Dimension–reduced geometry.

for the elastic stress  $\sigma$ . The parameters  $\lambda$  and  $\mu$  are the well-known Lamé coefficients. In a poroelastic medium, internal forces result from the elastic stress  $\sigma$  and the isotropic fluid pressure  $p^\Omega \mathbb{I}$ , where  $\mathbb{I}$  is the  $d \times d$  identity tensor. Their equilibrium is described by the Biot equation

$$-\mathbf{div}(\sigma(\mathbf{u}) - p^\Omega \mathbb{I}) = \mathbf{f}_E,$$

where  $\mathbf{f}_E$  denotes a volume force acting on the medium. We omit the possible dependence of the matrix permeability on the deformation field.

We formulate coupling conditions for the bulk–fracture interface based on conservation of momentum. As the fracture is supposed to be empty as far as mechanical behavior is concerned, there is no displacement variable in the fracture. Consequently, we cannot require continuity of the displacement at the interface. We therefore only postulate equality of the normal components of the total stress, which is  $p^f \mathbb{I}$  in the fracture and  $\sigma(\mathbf{u}) - p^\Omega \mathbb{I}$  in the surrounding matrix:

$$\sigma(\mathbf{u})\nu_f - p^\Omega \nu_f = -p^f \nu_f \quad (5)$$

on  $\partial\Omega_e \cap \partial\Omega_f$ . The continuity of pressure (3) then yields the boundary condition  $\sigma(\mathbf{u})\nu_f = \mathbf{0}$  on the interface.

## 2.2 Dimension Reduction of the Fracture

Fractures are typically long and thin objects. Following [23], we therefore replace the  $d$ –dimensional fracture by a  $(d-1)$ –dimensional hypersurface, and the equations on  $\Omega_f$  by reduced equations obtained by integrating (2) across the fracture thickness. The coupling conditions are modified accordingly. Unlike [23], we take the curvature of the fracture midsurface into account.

For the rest of this article we suppose that there is a parametrized hypersurface  $\Sigma$  (called the fracture midsurface) such that the fracture domain  $\Omega_f \subset \tilde{\Omega}$  can be represented by

$$\Omega_f = \left\{ \mathbf{x} \in \tilde{\Omega} \mid \mathbf{x} = \mathbf{s} + t\nu, \mathbf{s} \in \Sigma, t \in \left( -\frac{b(\mathbf{s})}{2}, \frac{b(\mathbf{s})}{2} \right) \right\},$$

where  $\nu$  denotes a continuous unit normal vector field to  $\Sigma$ , and  $b : \Sigma \rightarrow (0, \infty)$  is the fracture aperture function (Figure 2). The new bulk domain is  $\Omega := \tilde{\Omega} \setminus \Sigma$ , with outer boundary  $\Gamma := \partial\Omega \setminus \Sigma$ .

We distinguish two cases. Either, the fracture  $\Sigma$  partitions  $\tilde{\Omega}$  into two disconnected subdomains. In that case, we suppose that the two domains both have Lipschitz boundary, and we label them  $\Omega^+$  and  $\Omega^-$ , respectively. In the other case,  $\Omega$  is connected, which implies that at least parts of the fracture

boundary  $\gamma := \partial\Sigma$  are contained in  $\Omega$ . We then suppose that there exists a tangential extension  $\Sigma_e$  of  $\Sigma$  such that  $\tilde{\Sigma} := \Sigma \cup \Sigma_e$  subdivides  $\tilde{\Omega}$  into two disjoint subdomains  $\Omega^+$  and  $\Omega^-$  with Lipschitz-boundaries. In either way we denote the boundaries of  $\Omega^+$  and  $\Omega^-$  by  $\Gamma^+$  and  $\Gamma^-$ , respectively. We denote by  $\nu^\pm$  the unit outer normal to  $\Sigma^\pm := \Gamma^\pm \cap \tilde{\Sigma}$  and by  $\mathbf{n}$  the unit outer normal to the outer boundaries  $\Gamma^\pm \setminus \tilde{\Sigma}$ . To be specific, we set  $\nu := \nu^- = -\nu^+$ .

Dimension reduction of the fracture equation (2) involves splitting up the equation into normal and tangential parts. The projection operators onto the normal and tangent spaces of the parametrized hypersurface  $\Sigma$  are denoted by  $\mathbb{P}_\nu := \nu\nu^T$  and  $\mathbb{P}_\tau := \mathbb{I} - \mathbb{P}_\nu$ , respectively. For scalar-valued or vector-valued functions  $g$  and  $\mathbf{g}$ , we define the normal derivative by  $\nabla_\nu g := \nabla g \mathbb{P}_\nu$  and  $\nabla_\nu \mathbf{g} := \nabla \mathbf{g} \mathbb{P}_\nu$ , respectively. The normal divergence operator  $\text{div}_\nu$  is

$$\text{div}_\nu \mathbf{g} := \text{trace}(\nabla_\nu \mathbf{g}) = \mathbb{P}_\nu : \nabla \mathbf{g}.$$

The tangential gradient  $\nabla_\tau$  and divergence  $\text{div}_\tau$  are defined analogously. Finally, we introduce the average and the jump operator on  $\Sigma$  by

$$\{g\} := \frac{1}{2} (g|_{\Sigma^+} + g|_{\Sigma^-}) \quad \text{and} \quad [[g]] := (g|_{\Sigma^+} - g|_{\Sigma^-}),$$

respectively.

Suppose that the fracture permeability tensor  $\mathbb{K}^f$  decomposes additively as  $\mathbb{K}^f = K^\nu \mathbb{P}_\nu + K^\tau \mathbb{P}_\tau$  with constants  $K^\nu, K^\tau > 0$ . Then Equation (2b) can be decoupled into tangential and normal parts

$$\mathbb{P}^\tau \mathbf{q}^f = -K^\tau \nabla_\tau p^f, \quad (6a)$$

$$\mathbb{P}^\nu \mathbf{q}^f = -K^\nu \nabla_\nu p^f. \quad (6b)$$

Define the averaged fracture pressure  $p^\Sigma$  and the averaged tangential seepage velocity  $\mathbf{q}^\Sigma$  by

$$p^\Sigma(\mathbf{s}) := \frac{1}{b(\mathbf{s})} \int_{-\frac{b(\mathbf{s})}{2}}^{\frac{b(\mathbf{s})}{2}} p^f(\mathbf{s} + t\nu) \, dt \quad \text{and} \quad \mathbf{q}^\Sigma(\mathbf{s}) := \frac{1}{b(\mathbf{s})} \int_{-\frac{b(\mathbf{s})}{2}}^{\frac{b(\mathbf{s})}{2}} \mathbb{P}^\tau(\mathbf{s}) \mathbf{q}^f(\mathbf{s} + t\nu) \, dt.$$

The aim is to express equations (2a), (6a) and (6b) in terms of these averaged quantities. Simple calculations show that

$$\text{div} \mathbf{q}^f = \text{div}_\nu \mathbf{q}^f + \text{div}_\tau \mathbf{q}^\tau + \text{div}_\tau \mathbf{q}^\nu = \text{div}_\nu \mathbf{q}^f + \text{div}_\tau \mathbf{q}^\tau + \kappa \mathbf{q}^f \cdot \nu,$$

where  $\kappa = \text{div}_\tau \nu$  is the mean curvature of  $\Sigma$ ,  $\mathbf{q}^\nu := \mathbb{P}^\nu \mathbf{q}^f$  and  $\mathbf{q}^\tau := \mathbb{P}^\tau \mathbf{q}^f$ . Let  $\mathbf{s} \in \Sigma$  be arbitrary. In a first step, we integrate the left-hand side of (2a) in normal direction, and apply the Gauss and Leibniz integral rules to obtain

$$\begin{aligned} \int_{-\frac{b(\mathbf{s})}{2}}^{\frac{b(\mathbf{s})}{2}} \text{div} \mathbf{q}^f(\mathbf{s} + t\nu) \, dt &= \int_{-\frac{b(\mathbf{s})}{2}}^{\frac{b(\mathbf{s})}{2}} \text{div}_\nu \mathbf{q}^f(\mathbf{s} + t\nu) \, dt + \int_{-\frac{b(\mathbf{s})}{2}}^{\frac{b(\mathbf{s})}{2}} \text{div}_\tau \mathbf{q}^\tau(\mathbf{s} + t\nu) \, dt \\ &\quad + \int_{-\frac{b(\mathbf{s})}{2}}^{\frac{b(\mathbf{s})}{2}} \kappa(\mathbf{s}) \mathbf{q}^f(\mathbf{s} + t\nu) \cdot \nu(\mathbf{s}) \, dt \\ &= \left[ \mathbf{q}^f\left(\mathbf{s} + \frac{b(\mathbf{s})}{2}\nu\right) - \mathbf{q}^f\left(\mathbf{s} - \frac{b(\mathbf{s})}{2}\nu\right) \right] \cdot \nu(\mathbf{s}) \end{aligned} \quad (7)$$

$$+ \text{div}_\tau \int_{-\frac{b(\mathbf{s})}{2}}^{\frac{b(\mathbf{s})}{2}} \mathbf{q}^\tau(\mathbf{s} + t\nu) \, dt \quad (8)$$

$$-\frac{1}{2} \left( \mathbf{q}^\tau \left( \mathbf{s} - \frac{b(\mathbf{s})}{2} \nu \right) + \mathbf{q}^\tau \left( \mathbf{s} + \frac{b(\mathbf{s})}{2} \nu \right) \right) \cdot \nabla_\tau b(\mathbf{s}) \quad (9)$$

$$+ \kappa(\mathbf{s}) \int_{-\frac{b(\mathbf{s})}{2}}^{\frac{b(\mathbf{s})}{2}} \mathbf{q}^\nu(\mathbf{s} + t\nu) \, dt \cdot \nu(\mathbf{s}). \quad (10)$$

To simplify the first term (7), note that it only involves values of  $\mathbf{q}^\nu$  on the fracture boundary  $\partial\Omega_f \cap \partial\Omega_e$ . The continuity of fluxes (4) then yields

$$\mathbf{q}^f \left( \mathbf{s} \pm \frac{b(\mathbf{s})}{2} \nu(\mathbf{s}) \right) \cdot \nu(\mathbf{s}) = \mathbf{q}^\Omega \left( \mathbf{s} \pm \frac{b(\mathbf{s})}{2} \nu(\mathbf{s}) \right) \cdot \nu(\mathbf{s}). \quad (8b)$$

Since  $b$  is assumed to be small, we use the continuity of fluxes (8b) to approximate  $\mathbf{q}^\Omega \left( \mathbf{s} + \frac{b(\mathbf{s})}{2} \nu(\mathbf{s}) \right) \cdot \nu(\mathbf{s})$  by  $\mathbf{q}^\Omega(\mathbf{s})|_{\Sigma^+} \cdot \nu(\mathbf{s})$  and  $\mathbf{q}^\Omega \left( \mathbf{s} - \frac{b(\mathbf{s})}{2} \nu(\mathbf{s}) \right) \cdot \nu(\mathbf{s})$  by  $\mathbf{q}^\Omega(\mathbf{s})|_{\Sigma^-} \cdot \nu(\mathbf{s})$ . Together, this yields

$$\left[ \mathbf{q}^f \left( \mathbf{s} + \frac{b(\mathbf{s})}{2} \nu \right) - \mathbf{q}^f \left( \mathbf{s} - \frac{b(\mathbf{s})}{2} \nu \right) \right] \cdot \nu(\mathbf{s}) \approx \llbracket \mathbf{q}^\Omega \rrbracket(\mathbf{s}) \cdot \nu(\mathbf{s}).$$

To rewrite (9), define

$$\tilde{\mathbf{q}}^\tau(\mathbf{s}) := \frac{1}{2} \left( \mathbf{q}^\tau \left( \mathbf{s} - \frac{b(\mathbf{s})}{2} \nu \right) + \mathbf{q}^\tau \left( \mathbf{s} + \frac{b(\mathbf{s})}{2} \nu \right) \right).$$

Applying the trapezoidal rule and the continuity of the normal flux (8b) to the integral in (10) gives

$$\int_{-\frac{b(\mathbf{s})}{2}}^{\frac{b(\mathbf{s})}{2}} \mathbf{q}^\nu(\mathbf{s} + t\nu) \, dt \cdot \nu(\mathbf{s}) \approx b(\mathbf{s}) \{ \mathbf{q}^\nu \}(\mathbf{s}) \cdot \nu(\mathbf{s}) = b(\mathbf{s}) \{ \mathbf{q}^\Omega \}(\mathbf{s}) \cdot \nu(\mathbf{s}).$$

Finally, observe that the integral in (8) is simply  $b\mathbf{q}^\Sigma$ . In total, the divergence of  $\mathbf{q}^f$  is represented by

$$\int_{-\frac{b(\mathbf{s})}{2}}^{\frac{b(\mathbf{s})}{2}} \operatorname{div} \mathbf{q}^f(\mathbf{s} + t\nu) \, dt \approx \llbracket \mathbf{q}^\Omega \rrbracket(\mathbf{s}) \cdot \nu(\mathbf{s}) + \operatorname{div}_\tau(b(\mathbf{s})\mathbf{q}^\Sigma(\mathbf{s})) - \tilde{\mathbf{q}}^\tau(\mathbf{s}) \cdot \nabla_\tau b(\mathbf{s}) + b(\mathbf{s})\kappa(\mathbf{s}) \{ \mathbf{q}^\Omega \}(\mathbf{s}) \cdot \nu(\mathbf{s}).$$

Similarly, since  $K^\tau$  is constant, integrating the right-hand side of equation (6a) yields

$$\int_{-\frac{b(\mathbf{s})}{2}}^{\frac{b(\mathbf{s})}{2}} -K^\tau \nabla_\tau p^f(\mathbf{s} + t\nu) \, dt \approx -K^\tau (\nabla_\tau (bp^\Sigma) - \{p^\Omega\} \nabla_\tau b) = -K^\tau [b \nabla_\tau (p^\Sigma) - (\{p^\Omega\} - p^\Sigma) \nabla_\tau b],$$

where we have used the continuity of the pressure  $p^f = p^\Omega$ . Assuming that  $\nabla_\tau b$  is small, this yields

$$\begin{aligned} \operatorname{div}_\tau (b\mathbf{q}^\Sigma) &= b f^\Sigma - \llbracket \mathbf{q}^\Omega \rrbracket \cdot \nu - b\kappa \{ \mathbf{q}^\Omega \} \cdot \nu, \\ \mathbf{q}^\Sigma &= -K^\tau \nabla_\tau p^\Sigma, \end{aligned}$$

on  $\Sigma$ , where for any  $\mathbf{s} \in \Sigma$  we define

$$f^\Sigma(\mathbf{s}) := \frac{1}{b(\mathbf{s})} \int_{-\frac{b(\mathbf{s})}{2}}^{\frac{b(\mathbf{s})}{2}} f^f(\mathbf{s} + t\nu) \, dt.$$

Finally, we approximate the equation (6b) by integrating in normal direction. We use the trapezoidal rule, as before, for the left-hand side and apply the fundamental theorem of calculus to the right-hand side, to obtain

$$b \{ \mathbf{q}^\Omega \} \cdot \nu = -K^\nu \llbracket p^\Omega \rrbracket. \quad (11)$$

To close the system, we need to relate the fracture fluid pressure  $p^\Sigma$  to the bulk fluid pressure  $p^\Omega$  and the bulk flow  $\mathbf{q}^\Omega$ . To derive the corresponding formula, we will use the composite trapezoidal rule

$$\frac{1}{b(\mathbf{s})} \int_{-\frac{b(\mathbf{s})}{2}}^{\frac{b(\mathbf{s})}{2}} p^f(\mathbf{s} + t\nu) dt \approx \frac{1}{4} \left[ p^f\left(\mathbf{s} - \frac{b(\mathbf{s})}{2}\nu\right) + 2p^f(\mathbf{s}) + p^f\left(\mathbf{s} + \frac{b(\mathbf{s})}{2}\nu\right) \right]. \quad (12a)$$

We use the linear approximations

$$\begin{aligned} p^f(\mathbf{s}) &\approx p^f\left(\mathbf{s} + \frac{b(\mathbf{s})}{2}\nu\right) - \frac{b(\mathbf{s})}{2} \nabla p^f\left(\mathbf{s} + \frac{b(\mathbf{s})}{2}\nu\right) \cdot \nu(\mathbf{s}) \\ &= p^f\left(\mathbf{s} + \frac{b(\mathbf{s})}{2}\nu\right) + \frac{b(\mathbf{s})}{2K^\nu} \mathbf{q}^f\left(\mathbf{s} + \frac{b(\mathbf{s})}{2}\nu\right) \cdot \nu(\mathbf{s}). \end{aligned}$$

By symmetry, we can also write

$$p^f(\mathbf{s}) \approx p^f\left(\mathbf{s} - \frac{b(\mathbf{s})}{2}\nu\right) - \frac{b(\mathbf{s})}{2K^\nu} \mathbf{q}^f\left(\mathbf{s} - \frac{b(\mathbf{s})}{2}\nu\right) \cdot \nu(\mathbf{s}).$$

Averaging these two expressions yields the approximation

$$p^f(\mathbf{s}) \approx \frac{1}{2} \left[ p^f\left(\mathbf{s} - \frac{b(\mathbf{s})}{2}\nu\right) + p^f\left(\mathbf{s} + \frac{b(\mathbf{s})}{2}\nu\right) \right] \quad (12b)$$

$$+ \frac{b(\mathbf{s})}{2K^\nu} \left[ \mathbf{q}^f\left(\mathbf{s} + \frac{b(\mathbf{s})}{2}\nu\right) - \mathbf{q}^f\left(\mathbf{s} - \frac{b(\mathbf{s})}{2}\nu\right) \right] \cdot \nu(\mathbf{s}). \quad (12b)$$

By the continuity of the pressure and the fluxes on  $\partial\Omega_f \cap \partial\Omega_e$  and the approximations  $p^\Omega|_{\partial\Omega_f \cap \partial\Omega^\pm} \approx p^\Omega|_{\Sigma^\pm}$  and  $\mathbf{q}^\Omega \cdot \nu|_{\partial\Omega_f \cap \partial\Omega^\pm} \approx \mathbf{q}^\Omega \cdot \nu|_{\Sigma^\pm}$  it then follows that

$$\begin{aligned} p^\Sigma(\mathbf{s}) &= \frac{1}{b(\mathbf{s})} \int_{-\frac{b(\mathbf{s})}{2}}^{\frac{b(\mathbf{s})}{2}} p^f(\mathbf{s} + t\nu) dt \approx \frac{1}{4} \left[ 4 \{p^\Omega\}(\mathbf{s}) + 2 \frac{b(\mathbf{s})}{4K^\nu} \llbracket \mathbf{q}^\Omega \rrbracket(\mathbf{s}) \cdot \nu(\mathbf{s}) \right] \\ &= \{p^\Omega\}(\mathbf{s}) + \frac{b(\mathbf{s})}{8K^\nu} \llbracket \mathbf{q}^\Omega \rrbracket(\mathbf{s}) \cdot \nu(\mathbf{s}). \end{aligned}$$

This equation is a special case of the more general form

$$p^\Sigma = \{p^\Omega\} + (2\xi - 1) \frac{b}{4K^\nu} \llbracket \mathbf{q}^\Omega \rrbracket \cdot \nu \quad (12)$$

used in [23], where  $\xi \in (\frac{1}{2}, 1]$  depends on the choice of the discretization of the integral in the definition of  $p^\Sigma$ . The trapezoidal rule yields  $\xi = 1/2$ . With the composite trapezoidal rule (12a) and the averaged expression (12b), we have  $\xi = 3/4$ .

### 2.3 The Fully Coupled Problem with the Reduced Fracture Equation

Combining the dimension-reduced fracture fluid equations with the bulk flow and poroelasticity equation of the previous section, we arrive at the following problem: Find a fracture fluid pressure  $p^\Sigma : \Sigma \rightarrow \mathbb{R}$ , a bulk fluid pressure  $p^\Omega : \Omega \rightarrow \mathbb{R}$ , and a bulk displacement  $\mathbf{u} : \Omega \rightarrow \mathbb{R}^d$  such that

$$-\operatorname{div}(\sigma(\mathbf{u}) - p^\Omega \mathbb{I}) = \mathbf{f}_E \quad \text{in } \Omega \quad (13a)$$

$$\operatorname{div} \mathbf{q}^\Omega = f_F^\Omega \quad \text{in } \Omega, \quad (13b)$$

$$\mathbf{q}^\Omega = -\mathbb{K}^\Omega \nabla p^\Omega \quad \text{in } \Omega, \quad (13c)$$

$$\operatorname{div}_\tau (b \mathbf{q}^\Sigma) = b f_F^\Sigma - \llbracket \mathbf{q}^\Omega \rrbracket \cdot \nu - b \kappa \{ \mathbf{q}^\Omega \} \cdot \nu \quad \text{on } \Sigma, \quad (13d)$$

$$\mathbf{q}^\Sigma = -K^\tau \nabla_\tau p^\Sigma \quad \text{on } \Sigma. \quad (13e)$$

The first equation is the momentum balance of poroelasticity, followed by two equations for the matrix Darcy flow and two equations for the reduced fracture Darcy flow. The three processes are coupled partly by source terms in the equations themselves, and partly by explicit coupling conditions. In particular, the matrix fluid pressure  $p^\Omega$  appears in the poroelastic momentum balance (13a). The fluid flow  $\mathbf{q}^\Omega$  from the bulk to the fracture appears as a volume term in the fracture Darcy flow equation (13d). Conversely, by (11) and (12), the fracture fluid pressure  $p^\Sigma$  acts as Robin-type boundary condition for the bulk flow  $\mathbf{q}^\Omega$ :

$$p^\Sigma = \{ p^\Omega \} + (2\xi - 1) \frac{b}{4K^\nu} \llbracket \mathbf{q}^\Omega \rrbracket \cdot \nu \quad \text{on } \Sigma, \quad (14a)$$

$$\{ \mathbf{q}^\Omega \} \cdot \nu = -\frac{K^\nu}{b} \llbracket p^\Omega \rrbracket \quad \text{on } \Sigma. \quad (14b)$$

It acts as a Neumann boundary condition for the poroelastic equation

$$\sigma(\mathbf{u}|_{\Sigma^\pm}) \cdot \nu^\pm = -p^\Sigma \nu^\pm \quad (14c)$$

by the continuity of the total stress (5). Finally, the displacement  $\mathbf{u}$  determines the width of the fracture. In the reduced model, this width appears only in form of the fracture aperture function  $b : \Sigma \rightarrow \mathbb{R}$ . In a linear elastic setting it is reasonable to set the fracture width equal to the normal jump of the displacement field. We therefore impose the coupling condition

$$b = \llbracket \mathbf{u} \rrbracket \cdot \nu \quad \text{on } \Sigma. \quad (14d)$$

This is the ‘‘difficult’’ coupling condition which makes the coupled system nonlinear and possibly degenerate.

The system is closed using appropriate Dirichlet and Neumann boundary conditions for all three subsystems. Let  $\Gamma_N^E$  and  $\Gamma_D^E$  be two disjoint sets with  $\Gamma_N^E \cup \Gamma_D^E = \Gamma \setminus \gamma$ . For the displacement we have the boundary conditions

$$\sigma(\mathbf{u}) \cdot \mathbf{n} = \sigma_N \quad \text{on } \Gamma_N^E, \quad (15a)$$

$$\mathbf{u} = \mathbf{u}_D \quad \text{on } \Gamma_D^E, \quad (15b)$$

for given boundary data functions  $\sigma_N$  and  $\mathbf{u}_D$ . Similarly, let  $\Gamma_N^F$  and  $\Gamma_D^F$  be two disjoint sets with  $\Gamma_N^F \cup \Gamma_D^F = \Gamma \setminus \gamma$  and let  $q_N^\Omega$  and  $p_D^\Omega$  be given data. The bulk flow boundary conditions are

$$\mathbf{q}^\Omega \cdot \mathbf{n} = q_N^\Omega \quad \text{on } \Gamma_N^F, \quad (15c)$$

$$p^\Omega = p_D^\Omega \quad \text{on } \Gamma_D^F. \quad (15d)$$

Finally, the reduced fracture flow problem needs boundary conditions of  $\Sigma$ . Generally, the boundary of  $\Sigma$  is in part a subset of the domain boundary  $\partial\bar{\Omega}$  and in part contained in the interior of  $\bar{\Omega}$  (the fracture tip). We define the two disjoint sets  $\gamma_N^F$  and  $\gamma_D^F$  with  $\gamma_N^F \cup \gamma_D^F = \gamma$  and set the boundary conditions

$$\mathbf{q}^\Sigma \cdot \tau = q_N^\Sigma \quad \text{on } \gamma_N^F, \quad (15e)$$

$$p^\Sigma = p_D^\Sigma \quad \text{on } \gamma_D^F. \quad (15f)$$

### 3 Sobolev Spaces for the Bulk–Fracture System

Standard existence theory for the Darcy equation requires the permeability to be bounded from below away from zero almost everywhere. Unfortunately, this assumption does not hold if the fracture ends in the interior of the bulk domain, because coupling condition (14d) forces the fracture width  $b$  to tend to zero when approaching a crack tip. For a rigorous existence theory we therefore have to resort to weighted Sobolev spaces.

#### 3.1 Sobolev Spaces on Domains with a Slit

The bulk elasticity and fluid problems are posed on a domain with a slit. Solutions of elliptic equations on such domains are usually not first-order Sobolev functions. Instead, we construct certain weighted Sobolev spaces in which elliptic problems become well-posed.

Remember that the fracture domain  $\Sigma$  (possibly with extension  $\Sigma_e$ ) divides the domain  $\Omega$  into two Lipschitz domains  $\Omega^+$  and  $\Omega^-$ . Let  $L^2(\Omega^\pm)$  and  $H^1(\Omega^\pm)$  be the standard Lebesgue and Sobolev spaces on  $\Omega^\pm$ , with the norms  $\|\cdot\|_{0,\Omega^\pm}$  and  $\|\cdot\|_{1,\Omega^\pm}$ , and scalar products  $(\cdot, \cdot)_{0,\Omega^\pm}$  and  $(\cdot, \cdot)_{1,\Omega^\pm}$ , respectively. We then define

$$\tilde{V} = \left\{ v \in L^2(\Omega) \mid v|_{\Omega^\pm} \in H^1(\Omega^\pm) \right\},$$

and the broken scalar product

$$(\cdot, \cdot)_{\tilde{V}} : \tilde{V} \times \tilde{V} \rightarrow \mathbb{R}, \quad (u, v)_{\tilde{V}} := (u, v)_{H^1(\Omega^-)} + (u, v)_{H^1(\Omega^+)}.$$

The space  $\tilde{V}$  is a Hilbert space, and the induced norm is

$$\|\cdot\|_{1,\Omega}^2 := (\cdot, \cdot)_{\tilde{V}} = \|\cdot\|_{1,\Omega^-}^2 + \|\cdot\|_{1,\Omega^+}^2.$$

For any  $(d-1)$ -dimensional Lipschitz manifold  $M$  we denote the standard Sobolev–Slobodeckij space on  $M$  by  $H^{\frac{1}{2}}(M)$  (see, e.g., [36]) and the corresponding norm by  $\|\cdot\|_{\frac{1}{2},M}^2 := \|\cdot\|_{0,M}^2 + |\cdot|_{\frac{1}{2},M}^2$ , where  $|\cdot|_{\frac{1}{2},M}^2$  is the seminorm induced by the symmetric bilinear form

$$(u, v)_{\frac{1}{2},M} := \int_M \int_M \frac{|u(\mathbf{s}) - u(\tilde{\mathbf{s}})| |v(\mathbf{s}) - v(\tilde{\mathbf{s}})|}{|\mathbf{s} - \tilde{\mathbf{s}}|^d} \, d\mathbf{s} \, d\tilde{\mathbf{s}}.$$

Since  $\Omega^+$  and  $\Omega^-$  are Lipschitz domains there exist unique linear and continuous trace operators from  $H^1(\Omega^\pm)$  onto  $H^{\frac{1}{2}}(\Gamma^\pm)$ . We need their restrictions to the outer boundary  $\Gamma$  and the extended slit  $\tilde{\Sigma}$ .

**Definition 1.** Denote by  $\gamma_\Gamma : \tilde{V} \rightarrow H^{\frac{1}{2}}(\Gamma)$ ,  $\gamma^+ : H^1(\Omega^+) \rightarrow H^{\frac{1}{2}}(\tilde{\Sigma})$  and  $\gamma^- : H^1(\Omega^-) \rightarrow H^{\frac{1}{2}}(\tilde{\Sigma})$  the restrictions of the global trace operators from  $H^1(\Omega^\pm)$  onto  $H^{\frac{1}{2}}(\Gamma^\pm)$  to  $\Gamma$  and  $\tilde{\Sigma}$ .

In particular the jump and average operators  $[[\cdot]], \{\cdot\} : \tilde{V} \rightarrow H^{\frac{1}{2}}(\tilde{\Sigma})$ , given by

$$[[v]]_{\tilde{\Sigma}} := (\gamma^+ v - \gamma^- v) \quad \text{and} \quad \{v\}_{\tilde{\Sigma}} := \frac{1}{2} (\gamma^+ v + \gamma^- v),$$

are well defined, linear and continuous. The restrictions of these operators to  $\Sigma$  will be denoted by  $[[\cdot]]$  and  $\{\cdot\}$  (without a subscript), respectively.

Functions in  $\tilde{V}$  can have arbitrary jumps across the entire extended fracture  $\tilde{\Sigma}$ . To single out the functions that only jump at the actual interface  $\Sigma$  we now define the subspace

$$V := \left\{ v \in \tilde{V} \mid [[v]]_{\Sigma_e} = 0 \text{ almost everywhere} \right\}.$$

By the continuity of the trace operators it follows that  $V$  is a closed subspace of  $\tilde{V}$ . This is the usual definition of a first-order Sobolev Space on the non-Lipschitz domain  $\Omega \setminus \Sigma$ .

We now discuss the space of traces on  $\Sigma$  of function from  $V$ . Define the subspace  $H_0^{\frac{1}{2}}(\Sigma)$  of  $H^{\frac{1}{2}}(\Sigma)$  as the completion of  $C^{1,1}(\Sigma)$  with compact support in the  $H^{\frac{1}{2}}$ -norm. Let the extension of any  $v \in H_0^{\frac{1}{2}}(\Sigma)$  by 0 be denoted by  $\tilde{v}$ , i.e.,

$$\tilde{v} = \begin{cases} v & \text{on } \Sigma, \\ 0 & \text{on } \Sigma_e. \end{cases}$$

This extension  $\tilde{v}$  is not generally in  $H^{\frac{1}{2}}(\tilde{\Sigma})$  [20]. The subspace of functions in  $H_0^{\frac{1}{2}}$  whose extensions are in  $H^{\frac{1}{2}}(\tilde{\Sigma})$  is called

$$H_{00}^{\frac{1}{2}}(\Sigma) := \left\{ v \in H_0^{\frac{1}{2}}(\Sigma) \mid \tilde{v} \in H^{\frac{1}{2}}(\tilde{\Sigma}) \right\}.$$

Let  $d : \Sigma \rightarrow \mathbb{R}$  denote the geodesic distance of  $\mathbf{s} \in \Sigma$  to  $\gamma \cap \tilde{\Omega}$ . We define a scalar product  $(\cdot, \cdot)_{00,\Sigma} : H_{00}^{\frac{1}{2}}(\Sigma) \times H_{00}^{\frac{1}{2}}(\Sigma) \rightarrow \mathbb{R}$  by

$$(u, v)_{00,\Sigma} := (u, v)_{0,\Sigma} + (u, v)_{\frac{1}{2},\Sigma} + (u d^{-1/2}, v d^{-1/2})_{0,\Sigma}.$$

The space  $H_{00}^{\frac{1}{2}}(\Sigma)$  equipped with this scalar product is a Hilbert space [20] with induced norm  $\|\cdot\|_{00,\frac{1}{2},\Sigma}$ . Furthermore, a function  $v$  is in  $H_{00}^{\frac{1}{2}}(\Sigma)$  if and only if the norm  $\|v\|_{00,\frac{1}{2},\Sigma}$  is finite [20].

We introduce the space of admissible traces

$$W_\Sigma := \left\{ (v^+, v^-) \in H^{\frac{1}{2}}(\Sigma) \times H^{\frac{1}{2}}(\Sigma) \mid (v^- - v^+) \in H_{00}^{\frac{1}{2}}(\Sigma) \right\}.$$

A norm on this space is

$$\|(v^-, v^+)\|^2 = \|v^-\|_{\frac{1}{2},\Sigma}^2 + \|v^+\|_{\frac{1}{2},\Sigma}^2 + \|(v^+ - v^-) d^{-1/2}\|_{0,\Sigma}^2.$$

The following result establishes a relation between the space  $V$  of Sobolev functions on the slit domain  $\Omega$ , and the space  $W_\Sigma$  of traces. It shows that  $W_\Sigma$  is the correct trace space of  $V$  on  $\Sigma$ .

**Lemma 2** ([20], Theorem 1.25).

- (i) *There exists a continuous linear trace operator  $\gamma_\Sigma : V \rightarrow W_\Sigma, v \mapsto (\gamma^- v, \gamma^+ v)$ .*
- (ii) *There exists a continuous linear extension operator  $E_\Sigma : W_\Sigma \rightarrow V, (v^-, v^+) \mapsto v$  such that  $\gamma_\Sigma \circ E_\Sigma = id$ .*

In particular, all traces of functions in  $V$  are  $H_{00}^{\frac{1}{2}}(\Sigma)$ -functions. All definitions in this section can

be made equally well for vector-valued spaces. Such spaces will be written in bold face. For  $d$ -valued spaces, we mention the following generalized Green's formula, which is proved in [2].

**Lemma 3.** *Let  $\Omega$  and  $\Sigma$  satisfy the conditions of Section 2.2. Let  $\mathbf{u} \in \mathbf{L}^2(\Omega)$  satisfy  $\operatorname{div} \mathbf{u} \in L^2(\Omega)$  and let  $v \in V$ . Then*

$$\int_{\Omega} (\operatorname{div} \mathbf{u}) v + \mathbf{u} \cdot \nabla v \, d\mathbf{x} = (\mathbf{u} \cdot \mathbf{n}, v)_{0,\Gamma} - (\llbracket \mathbf{u} \cdot \boldsymbol{\nu} \rrbracket, \{v\})_{0,\Sigma} - (\{u \cdot \boldsymbol{\nu}\}, \llbracket v \rrbracket)_{0,\Sigma}.$$

### 3.2 Weighted Lebesgue Spaces on Parametrized Hypersurfaces

In this section we will assume that the fracture width function  $b : \Sigma \rightarrow \mathbb{R}$  is fixed. The functions  $b$  and  $b^{-1}$  appear as degenerate and singular coefficients in the averaged fracture fluid equation (13d) and the fluid coupling conditions (14a), (14b). We must therefore resort to weighted Sobolev spaces on the fracture to obtain well-posed fluid problems. We recall the basic definitions.

**Definition 4.** Let  $\widehat{\omega} : \mathbb{R}^N \rightarrow \mathbb{R}$  be a function and let  $M \subset \mathbb{R}^N$  be open and bounded.

(i) The function  $\widehat{\omega}$  is called a weight if  $\widehat{\omega} \in L^1_{loc}(\mathbb{R}^N)$  and  $\widehat{\omega} > 0$  almost everywhere.

(ii) Let  $\widehat{\omega}$  be a weight. The weighted  $L^2$ -space  $L^2_{\widehat{\omega}}(M)$  is defined as

$$L^2_{\widehat{\omega}}(M) := \left\{ v : M \rightarrow \mathbb{R} \mid v \text{ is measurable, } \|v\|_{\widehat{\omega}, M} < \infty \right\},$$

where the norm

$$\|v\|_{\widehat{\omega}, M}^2 := \int_M |v|^2 \widehat{\omega} \, d\mathbf{x}$$

is induced by the weighted scalar product

$$(u, v)_{\widehat{\omega}, M} := \left( \widehat{\omega}^{\frac{1}{2}} u, \widehat{\omega}^{\frac{1}{2}} v \right)_{0, M}.$$

(iii) The space  $L^2_{\widehat{\omega}, 0}(M)$  is defined as the closure of  $C^\infty_0(M)$  in  $L^2_{\widehat{\omega}}(M)$ .

(iv) A weight  $\widehat{\omega}$  is called an  $A_2$ -weight if there exists a constant  $A > 0$  such that for all balls  $B$  in  $\mathbb{R}^N$  we have

$$\left( \frac{1}{|B|} \int_B \widehat{\omega}(\mathbf{x}) \, d\mathbf{x} \right) \left( \frac{1}{|B|} \int_B \widehat{\omega}(\mathbf{x})^{-1} \, d\mathbf{x} \right) \leq A,$$

independent of  $B$ .

If  $\widehat{\omega}$  is an  $A_2$ -weight, then  $L^2_{\widehat{\omega}}(M)$  and  $L^2_{\widehat{\omega}, 0}(M)$  are Banach spaces ([33], Proposition 2.1.2). Furthermore,  $C^\infty(M) \cap L^2_{\widehat{\omega}}(M)$  is then dense in  $L^2_{\widehat{\omega}}(M)$  ([25], Lemma 2.4).

We extend these definitions to parametrized hypersurfaces.

**Definition 5.** Let  $\Sigma \subset \mathbb{R}^d$  be a hypersurface defined by the homeomorphism  $\alpha : \Sigma \rightarrow \widehat{\Sigma} \subset \mathbb{R}^{d-1}$ .

(i) We call a function  $\omega : \Sigma \rightarrow \mathbb{R}$  a weight on  $\Sigma$  if there exists a weight  $\widehat{\omega} : \mathbb{R}^{d-1} \rightarrow \mathbb{R}$  such that  $\widehat{\omega}|_{\widehat{\Sigma}} = \omega \circ \alpha^{-1}$ .

(ii) Let  $\omega : \Sigma \rightarrow \mathbb{R}$  be a weight on  $\Sigma$ . We say that a function  $v : \Sigma \rightarrow \mathbb{R}$  belongs to  $L^2_{\omega}(\Sigma)$ , if  $v \circ \alpha^{-1} \in L^2_{\widehat{\omega}}(\widehat{\Sigma})$ .

(iii) Let  $\omega : \Sigma \rightarrow \mathbb{R}$  be a weight on  $\Sigma$ . We say that  $\omega$  is an  $A_2(\Sigma)$ -weight, if  $\widehat{\omega}$  is an  $A_2$ -weight.

Spaces of functions on parametrized hypersurfaces with  $A_2$ -weighted norms are Hilbert spaces.

**Theorem 6.** Let  $\Sigma$  be a hypersurface defined by the homeomorphism  $\alpha : \Sigma \rightarrow \widehat{\Sigma} \subset \mathbb{R}^{d-1}$  and  $\omega$  an  $A_2(\Sigma)$ -weight. The space  $L^2_{\omega}(\Sigma)$  equipped with the norm

$$\|v\|_{0, \omega, \Sigma}^2 := \|v \circ \alpha^{-1}\|_{0, \widehat{\omega}, \widehat{\Sigma}}^2$$

is a separable Hilbert space. The norm is induced by the scalar product

$$(u, v)_{\omega, \Sigma} := \left( \widehat{\omega}^{\frac{1}{2}} (u \circ \alpha^{-1}), \widehat{\omega}^{\frac{1}{2}} (v \circ \alpha^{-1}) \right)_{0, \alpha[\widehat{\Sigma}]}.$$

Furthermore,  $C^\infty(\Sigma) \cap L^2_{\omega}(\Sigma)$  is dense in  $L^2_{\omega}(\Sigma)$ .

*Proof.* It is easy to see that the norm  $\|\cdot\|_{0,\omega,\Sigma}$  is induced by the scalar product  $(\cdot, \cdot)_{\omega,\Sigma}$ .

To show the completeness of  $L^2_\omega(\Sigma)$ , let  $(v_n)_{n \in \mathbb{N}}$  be a Cauchy sequence in  $L^2_\omega(\Sigma)$ . Then the sequence  $(v_n \circ \alpha^{-1})_{n \in \mathbb{N}}$  is a Cauchy sequence in  $L^2_\omega(\widehat{\Sigma})$ . Since  $L^2_\omega(\widehat{\Sigma})$  is complete, there exists a  $\widehat{v} \in L^2_\omega(\widehat{\Sigma})$  with  $v_n \circ \alpha^{-1} \rightarrow \widehat{v}$  for  $n \rightarrow \infty$ . Define  $v := \widehat{v} \circ \alpha$ , then

$$\|v_n - v\|_{0,\omega,\Sigma} = \|(v_n - v) \circ \alpha^{-1}\|_{0,\widehat{\omega},\widehat{\Sigma}} = \|v_n \circ \alpha^{-1} - \widehat{v}\|_{0,\widehat{\omega},\widehat{\Sigma}} \rightarrow 0 \quad \text{for } n \rightarrow \infty.$$

This proves completeness.

Now, let  $v \in L^2_\omega(\Sigma)$  be a function. Then  $(v \circ \alpha^{-1}) \in L^2_\omega(\widehat{\Sigma})$ . Since  $L^2_\omega(\widehat{\Sigma}) \cap C^\infty(\widehat{\Sigma})$  is dense in  $L^2_\omega(\widehat{\Sigma})$ , there exists a sequence  $(\widehat{v}_n)_{n \in \mathbb{N}}$  in  $C^\infty(\widehat{\Sigma}) \cap L^2_\omega(\widehat{\Sigma})$  converging towards  $(v \circ \alpha^{-1})$  in  $L^2_\omega(\widehat{\Sigma})$ . For  $(v_n)_{n \in \mathbb{N}}$  defined by  $v_n := \widehat{v}_n \circ \alpha$  it follows that

$$\|v_n - v\|_{0,\omega,\Sigma} = \|(v_n - v) \circ \alpha^{-1}\|_{0,\widehat{\omega},\widehat{\Sigma}} = \|\widehat{v}_n - v \circ \alpha^{-1}\|_{0,\widehat{\omega},\widehat{\Sigma}} \rightarrow 0 \quad \text{for } n \rightarrow \infty.$$

□

We now construct weighted Lebesgue spaces using the fracture width function as our weight.

**Assumptions 7.** Let  $\Sigma$  be a hypersurface with boundary  $\gamma := \partial\Sigma$  defined by the homeomorphism  $\alpha : \Sigma \rightarrow \widehat{\Sigma}$ . We assume that  $b : \Sigma \rightarrow \mathbb{R}$  satisfies the following conditions:

A1 The function  $b$  is a weight on  $\Sigma$ .

A2 Let  $\chi$  be a smooth cutoff function with  $\chi = 1$  in a neighborhood of  $\gamma$ . There exists a constant  $c > 0$  such that the function  $b$  is given by

$$b = c(\chi \operatorname{dist}^{\frac{1}{2}} + (1 - \chi)f),$$

where  $f$  denotes an integrable function and  $\operatorname{dist} : \mathbb{R}^d \rightarrow \mathbb{R}$  denotes the distance in  $\mathbb{R}^d$  to  $\gamma$ .

A3 The function  $b$  is essentially bounded on  $\Sigma$  by a constant  $b_{\max} > 0$ .

A4 The function  $f$  is essentially bounded from below away from zero, i.e., there exists a constant  $a > 0$  such that  $a \leq f$  almost everywhere on  $\Sigma$ .

The crucial assumption A2 is motivated in Chapter 4 by asymptotic expansion of the matrix displacement field near the crack tip.

**Lemma 8.** Let  $\Sigma$  be a bounded hypersurface defined by the homeomorphism  $\alpha : \Sigma \rightarrow \widehat{\Sigma}$  with boundary  $\gamma = \partial\Sigma$ , and let  $b : \Sigma \rightarrow \mathbb{R}$  satisfy Assumptions A1-A4. Then  $b$  is an  $A_2(\Sigma)$ -weight.

*Proof.* We define  $F = \{\mathbf{s} \in \Sigma \mid \chi(\mathbf{s}) = 1\}$ . Since  $\operatorname{dist} > 0$  away from the crack tip, there exists a constant  $d_{\min} > 0$  such that  $d_{\min} \leq \operatorname{dist}^{\frac{1}{2}}$  on  $\Sigma \setminus F$ . With Assumption A3 it thus follows that

$$b \leq b_{\max} \leq \frac{b_{\max}}{d_{\min}} \operatorname{dist}^{\frac{1}{2}} \quad \text{on } \Sigma \setminus F.$$

Since  $b = c \operatorname{dist}^{\frac{1}{2}}$  on  $F$  we conclude that  $b \leq M \operatorname{dist}^{\frac{1}{2}}$  on  $\Sigma$ , where  $M := \max\left\{c, \frac{b_{\max}}{d_{\min}}\right\}$ . With Assumptions A2 and A4 it furthermore follows that

$$b = \chi \operatorname{dist}^{\frac{1}{2}} + (1 - \chi)f \geq \chi d_{\min} + (1 - \chi)a \geq \min\{d_{\min}, a\}$$

on  $\Sigma \setminus F$ . Since  $\Sigma$  is bounded, we can find a constant  $d_{\max} > 0$ , such that  $\operatorname{dist}^{\frac{1}{2}} \leq d_{\max}$  on  $\Sigma$ . This yields the estimate

$$b^{-1} \leq \frac{1}{\min\{d_{\min}, a\}} = \frac{1}{\min\{d_{\min}, a\}} \frac{d_{\max}}{d_{\max}} \leq \frac{d_{\max}}{\min\{d_{\min}, a\}} \operatorname{dist}^{-\frac{1}{2}}.$$

Since  $b^{-1} = c^{-1} \text{dist}^{-\frac{1}{2}}$  on  $F$ , we conclude that  $b^{-1} \leq m \text{dist}^{-\frac{1}{2}}$ , where  $m = \max \left\{ \frac{d_{\max}}{\min\{d_{\min}, a\}}, c^{-1} \right\}$ .

Let  $\widehat{d} : \mathbb{R}^{d-1} \rightarrow \mathbb{R}$  denote the distance of  $\mathbf{s} \in \mathbb{R}^{d-1}$  to the set  $\widehat{\gamma} := \partial\widehat{\Sigma}$ . The boundedness of  $\Sigma$  yields that there exist constants  $d, D > 0$ , such that  $d\widehat{d}(\mathbf{s})^{\frac{1}{2}} \leq \text{dist}(\alpha^{-1}(\mathbf{s}), \gamma)^{\frac{1}{2}} \leq D\widehat{d}(\mathbf{s})^{\frac{1}{2}}$  for all  $\mathbf{s} \in \widehat{\Sigma}$ .

Together with the previous estimates we get  $dm\widehat{d} \leq b \circ \alpha \leq DM\widehat{d}^{\frac{1}{2}}$  on  $\widehat{\Sigma}$ . Finally, by Lemma 3.3 in [9], it follows that the function  $\widehat{d}^{\frac{1}{2}}$  is an  $A_2$  weight, i.e., there exists a constant  $\widehat{A}$ , such that

$$\left( \frac{1}{|\widehat{B}|} \int_{\widehat{B}} \widehat{d} \, d\mathbf{s} \right)^{\frac{1}{2}} \left( \frac{1}{|\widehat{B}|} \int_{\widehat{B}} \widehat{d}^{-\frac{1}{2}} \, d\mathbf{s} \right) \leq \widehat{A}$$

independent of the choice of the ball  $\widehat{B} \subset \mathbb{R}^{d-1}$ .

Then the function  $\widehat{b}$  defined by

$$\widehat{b} := \begin{cases} b \circ \alpha^{-1} & \text{on } \widehat{\Sigma} \\ \widehat{d}^{\frac{1}{2}} & \text{otherwise} \end{cases}$$

satisfies for arbitrary balls  $\widehat{B}$  in  $\mathbb{R}^{d-1}$

$$\begin{aligned} \left( \frac{1}{|\widehat{B}|} \int_{\widehat{B}} \widehat{b} \, d\mathbf{s} \right) \left( \frac{1}{|\widehat{B}|} \int_{\widehat{B}} \widehat{b}^{-1} \, d\mathbf{s} \right) &= \frac{1}{|\widehat{B}|^2} \left( \int_{\widehat{B} \cap \widehat{\Sigma}} \widehat{b} \, d\mathbf{s} + \int_{\widehat{B} \setminus \widehat{\Sigma}} \widehat{b} \, d\mathbf{s} \right) \left( \int_{\widehat{B} \cap \widehat{\Sigma}} \widehat{b}^{-1} \, d\mathbf{s} + \int_{\widehat{B} \setminus \widehat{\Sigma}} \widehat{b}^{-1} \, d\mathbf{s} \right) \\ &\leq \frac{\max\{1, dm\} \max\{1, DM\}}{|\widehat{B}|^2} \left( \int_{\widehat{B}} \widehat{d}^{\frac{1}{2}} \, d\mathbf{s} \right) \left( \int_{\widehat{B}} \widehat{d}^{-\frac{1}{2}} \, d\mathbf{s} \right) \\ &\leq \max\{1, dm\} \max\{1, DM\} \widehat{A}. \end{aligned}$$

Hence, by Definition 5(iii),  $b$  is an  $A_2(\Sigma)$ -weight.  $\square$

As in the Euclidean case, the fact that  $b$  is an  $A_2$ -weight allows to conclude that the corresponding Lebesgue spaces have desirable properties.

**Lemma 9.** *Let  $\Sigma$  be a bounded hypersurface defined by the homeomorphism  $\alpha : \Sigma \rightarrow \widehat{\Sigma}$  with boundary  $\gamma = \partial\Sigma$ , and let  $b : \Sigma \rightarrow \mathbb{R}$  satisfy Assumptions A1-A4. Define the  $L_b^2(\Sigma)$  and  $L_{b^{-1}}^2(\Sigma)$  with the corresponding norms  $\|\cdot\|_{0,b,\Sigma}$  and  $\|\cdot\|_{0,b^{-1},\Sigma}$  as in Definition 5 and Theorem 6. Then the spaces  $L_b^2(\Sigma)$  and  $L_{b^{-1}}^2(\Sigma)$  are separable Hilbert spaces. We have the continuous embeddings*

$$L_{b^{-1}}^2(\Sigma) \hookrightarrow L^2(\Sigma) \hookrightarrow L_b^2(\Sigma).$$

*Proof.* The assumptions A1-A4 yield that  $b$  is an  $A_2$ -weight and  $L_b^2(\Sigma)$  is a separable Hilbert space by Theorem 6. By the symmetry of definition 4(iv),  $b^{-1}$  is an  $A_2$ -weight as well; which proves the assertion about  $L_{b^{-1}}^2(\Sigma)$ . The continuous embeddings exist because  $b$  is bounded from above.  $\square$

### 3.3 A Sobolev Space with Weighted Trace Space

In this section we will construct a Sobolev space representing the volume pressure  $p^\Omega$ . Due to the coupling conditions (14), we need such a space to have its trace in

$$H_{b^{-1}}^{\frac{1}{2}}(\Sigma) := L_{b^{-1}}^2(\Sigma) \cap H^{\frac{1}{2}}(\Sigma).$$

To this end, we the norm

$$\|v\|_{\frac{1}{2}, b^{-1}, \Sigma}^2 := \|v\|_{0, b^{-1}, \Sigma}^2 + |v|_{\frac{1}{2}, \Sigma}^2.$$

From  $L_{b^{-1}}^2(\Sigma) \hookrightarrow L^2(\Sigma)$  and the definition of  $H_{b^{-1}}^{\frac{1}{2}}(\Sigma)$  it follows that  $H_{b^{-1}}^{\frac{1}{2}}(\Sigma) \hookrightarrow H^{\frac{1}{2}}(\Sigma)$ .

**Theorem 10.** *Let  $\Sigma$  be a bounded hypersurface defined by the homeomorphism  $\alpha : \Sigma \rightarrow \widehat{\Sigma}$  with boundary  $\gamma = \partial\Sigma$ , and let  $b : \Sigma \rightarrow \mathbb{R}$  satisfy Assumptions A1-A4. Then the space  $H_{b^{-1}}^{\frac{1}{2}}$  equipped with the norm  $\|\cdot\|_{\frac{1}{2}, b^{-1}, \Sigma}$  is a separable Hilbert space.*

*Proof.* The square of the norm  $\|\cdot\|_{\frac{1}{2}, b^{-1}, \Sigma}$  is the sum of squared norms that are induced by scalar products. Therefore  $\|\cdot\|_{\frac{1}{2}, b^{-1}, \Sigma}$  is induced by a scalar product as well.

Let  $(s_n)_{n \in \mathbb{N}}$  be a Cauchy sequence in  $H_{b^{-1}}^{\frac{1}{2}}(\Sigma)$ . Then  $(s_n)_{n \in \mathbb{N}}$  is a Cauchy sequence in the Hilbert space  $L_{b^{-1}}^2(\Sigma)$ . Hence there exists a  $s \in L_{b^{-1}}^2(\Sigma)$  with  $s_n \rightarrow s$  in  $L_{b^{-1}}^2(\Sigma)$ .

To prove completeness it remains to show that  $s \in H_{b^{-1}}^{\frac{1}{2}}(\Sigma)$ , i.e., that  $|s|_{\frac{1}{2}, \Sigma}$  is bounded and that  $|s_n - s|_{\frac{1}{2}, \Sigma} \rightarrow 0$ . But since  $L_{b^{-1}}^2(\Sigma) \hookrightarrow L^2(\Sigma)$  we can conclude from the corresponding result for  $H^{\frac{1}{2}}(\Sigma)$  ([36], Theorem 3.1) that both conditions are satisfied.

Finally, the space  $H_{b^{-1}}^{\frac{1}{2}}(\Sigma)$  can be identified with a closed subspace of the separable product space  $L_{b^{-1}}^2(\Sigma) \times L^2(\Sigma \times \Sigma)$ , which implies the separability of  $H_{b^{-1}}^{\frac{1}{2}}(\Sigma)$  (see [36], Theorem 3.1).  $\square$

The coupling constraints (14a) and (14b) require that the trace space on  $\Sigma$  of the volume pressure space should be  $H_{b^{-1}}^{\frac{1}{2}}(\Sigma)$ . Therefore we define

$$V_{b^{-1}} := \left\{ v \in V \mid \gamma^{\pm} v \in H_{b^{-1}}^{\frac{1}{2}}(\Sigma) \right\},$$

and equip this space with the norm

$$\|v\|_{1, b^{-1}, \Omega}^2 = \|\gamma^+ v\|_{0, b^{-1}, \Sigma}^2 + \|\gamma^- v\|_{0, b^{-1}, \Sigma}^2 + \|v\|_{1, \Omega}^2.$$

It is easy to see that  $V_{b^{-1}} \hookrightarrow V$ .

**Lemma 11.** *The restriction of  $\gamma_{\Gamma} : V \rightarrow H^{\frac{1}{2}}(\Gamma)$  from Definition 1 onto an operator from  $V_{b^{-1}}$  to  $H^{\frac{1}{2}}(\Gamma)$ , and the restrictions of  $\gamma^{\pm} : V \rightarrow H^{\frac{1}{2}}(\Sigma)$  from Definition 1 to operators from  $V_{b^{-1}}$  to  $H^{\frac{1}{2}}(\Sigma)$  are well defined, linear and continuous.*

*Proof.* The embedding  $V_{b^{-1}} \hookrightarrow V$  yields that the restriction of  $\gamma_{\Gamma} : V \rightarrow H^{\frac{1}{2}}(\Gamma)$  onto an operator from  $V_{b^{-1}}$  is well defined, linear and continuous.

Analogously, the restrictions of the trace operators  $\gamma^{\pm} : V \rightarrow H^{\frac{1}{2}}(\Sigma)$  onto operators from  $V_{b^{-1}}$  to  $H^{\frac{1}{2}}(\Sigma)$  are well defined and linear. By the definition of  $V_{b^{-1}}$  it follows that the restricted operators  $\gamma^{\pm}$  map onto  $H_{b^{-1}}^{\frac{1}{2}}(\Sigma)$ . Furthermore, for any  $v \in V_{b^{-1}}$  the following estimate is satisfied:

$$\begin{aligned} \|\gamma^+ v\|_{\frac{1}{2}, b^{-1}, \Sigma}^2 &= \|\gamma^+ v\|_{0, b^{-1}, \Sigma}^2 + |\gamma^+ v|_{\frac{1}{2}, \Sigma}^2 \\ &\leq \|\gamma^+ v\|_{0, b^{-1}, \Sigma}^2 + \|\gamma^+ v\|_{\frac{1}{2}, \Sigma}^2 \\ &\leq C \left( \|\gamma^+ v\|_{0, b^{-1}, \Sigma}^2 + \|v\|_{1, \Omega^+}^2 \right). \end{aligned}$$

Analogously one can show that  $\|\gamma^- v\|_{\frac{1}{2}, b^{-1}, \Sigma}^2 \leq C \left( \|\gamma^- v\|_{0, b^{-1}, \Sigma}^2 + \|v\|_{1, \Omega^-}^2 \right)$ . This proves continuity.  $\square$

As in Section 3.1, we introduce the space of admissible traces. Define

$$W_{b^{-1}} := \left\{ (v^-, v^+) \in H_{b^{-1}}^{\frac{1}{2}}(\Sigma) \times H_{b^{-1}}^{\frac{1}{2}}(\Sigma) \mid (v^+ - v^-) \in H_{00}^{\frac{1}{2}}(\Sigma) \right\}$$

with norm

$$\|(v^-, v^+)\|_{W_{b^{-1}}}^2 := \|\gamma^- v\|_{\frac{1}{2}, b^{-1}, \Sigma}^2 + \|\gamma^+ v\|_{\frac{1}{2}, b^{-1}, \Sigma}^2.$$

This norm is equivalent to the more natural choice

$$\|(v^+, v^-)\|^2 = \|v^-\|_{\frac{1}{2}, b^{-1}, \Sigma}^2 + \|v^+\|_{\frac{1}{2}, b^{-1}, \Sigma}^2 + \|(v^+ - v^-) d^{-1/2}\|_{0, \Sigma}^2,$$

since  $b^{-1}$  behaves like  $\text{dist}^{-\frac{1}{2}} \geq d^{-\frac{1}{2}}$  near the crack tip. This yields that there exists a constant  $C$  such that

$$\begin{aligned} \|(v^+ - v^-) d^{-1/2}\|_{0, \Sigma} &\leq \|v^+ d^{-1/2}\|_{0, \Sigma} + \|v^- d^{-1/2}\|_{0, \Sigma} \\ &\leq C \left( \|v^+\|_{0, b^{-1}, \Sigma} + \|v^-\|_{0, b^{-1}, \Sigma} \right). \end{aligned}$$

The next Lemma follows directly by the definitions of the spaces  $V_{b^{-1}}$  and  $W_{b^{-1}}$ .

**Lemma 12.**

- (i) *The restriction of the trace operator  $\gamma_\Sigma : V \rightarrow W_\Sigma$  from Lemma 2 onto an operator from  $V_{b^{-1}}$  to  $W_{b^{-1}}$  is well defined, linear and continuous.*
- (ii) *The restriction of the extension operator  $E_\Sigma : W_\Sigma \rightarrow V$  from Lemma 2 onto an operator from  $W_{b^{-1}}$  to  $V_{b^{-1}}$  is well defined, linear and continuous.*

*Proof.*

- (i) By Lemma 11 it follows that the Operator  $\gamma_\Sigma$  is linear and continuous. By the definition of  $V_{b^{-1}}$  (or more precisely: by the definition of  $V$ ) it follows that  $\llbracket v \rrbracket \in H_{00}^{\frac{1}{2}}(\Sigma)$ .
- (ii) By definition of  $W_{b^{-1}}$  it follows that for  $\tilde{v} = (v^-, v^+) \in W_{b^{-1}}$  we have  $v^\pm \in H_{b^{-1}}^{\frac{1}{2}}(\Sigma) \subset H^{\frac{1}{2}}(\Sigma)$ . Then the extension of  $\tilde{v}$  from Lemma 2 satisfies  $E_\Sigma \tilde{v} \in V$ . To show that  $E_\Sigma \tilde{v} \in V_{b^{-1}}$  it is required that  $\gamma_\Sigma(E_\Sigma \tilde{v}) \in H_{b^{-1}}^{\frac{1}{2}}(\Sigma)$ . But this is a direct consequence of Lemma 2, since  $\gamma_\Sigma \circ E_\Sigma = \text{id}$ .

□

**Theorem 13.** *The space  $V_{b^{-1}}$  equipped with the norm  $\|\cdot\|_{1, b^{-1}, \Omega}$  is a separable Hilbert space.*

*Proof.* Obviously the norm  $\|\cdot\|_{1, b^{-1}, \Omega}$  is induced by a scalar product.

By definition  $V$  is a Hilbert space and  $V_{b^{-1}}$  is a subspace of  $V$ . The space  $W_{b^{-1}}$  is a closed subspace of the space  $H_{b^{-1}}^{\frac{1}{2}}\Sigma \times H_{b^{-1}}^{\frac{1}{2}}(\Sigma)$ , which, by Theorem 10, is a separable Hilbert space. The linearity and continuity of the trace operator  $\gamma_\Sigma$  (Lemma 12) yields that  $V_{b^{-1}}$  is a Banach space with respect to the graph norm

$$\|v\|_G^2 := \|v\|_{1, \Omega}^2 + \|(\gamma^+ v, \gamma^- v)\|_{W_{b^{-1}}}^2.$$

The continuity of the trace operators (Lemma 11) yields the equivalence of the norm  $\|\cdot\|_G$  and  $\|\cdot\|_{1, b^{-1}, \Omega}$ , and hence completeness of  $V_{b^{-1}}$  with respect to the norm  $\|\cdot\|_{1, b^{-1}, \Omega}$ . Hence, the space  $V_{b^{-1}}$  is a closed subspace of the separable Hilbert space  $V$ , which again implies the separability of  $V_{b^{-1}}$ . □

Note that from  $\gamma^+ v^2 + \gamma^- v^2 = 2\{p\}^2 + \frac{1}{2}\llbracket p \rrbracket^2$  an equivalent formulation of the norm  $\|v\|_{1, b^{-1}, \Omega}^2$  is

$$\|v\|_{1, b^{-1}, \Omega}^2 = \frac{1}{2} \|\llbracket v \rrbracket\|_{0, b^{-1}, \Sigma}^2 + 2\|\{v\}\|_{0, b^{-1}, \Sigma}^2 + \|v\|_{1, \Omega}^2.$$

### 3.4 A Weighted Sobolev Space on the Fracture

We now introduce a space representing the averaged fracture pressure  $p^\Sigma$ , namely

$$H_b^1(\Sigma) := \{v \in L_{b^{-1}}^2(\Sigma) \mid \nabla_\tau v \in \mathbf{L}_b^2(\Sigma)\}.$$

This space is equipped with the norm

$$\|v\|_{1,b,\Sigma}^2 := \|v\|_{0,b^{-1},\Sigma}^2 + \|\nabla_\tau v\|_{0,b,\Sigma}^2.$$

**Theorem 14.** *Let  $\Sigma$  be a bounded hypersurface defined by the diffeomorphism  $\alpha : \Sigma \rightarrow \widehat{\Sigma}$  with boundary  $\gamma = \partial\Sigma$ , and let  $b : \Sigma \rightarrow \mathbb{R}$  satisfy Assumptions A1-A4. Then, the space  $H_b^1(\Sigma)$  equipped with the norm  $\|\cdot\|_{1,b,\Sigma}$  is a Hilbert space.*

*Proof.* It is easy to see that the norm is induced by the scalar products for  $L_{b^{-1}}^2(\Sigma)$  and  $\mathbf{L}_b^2(\Sigma)$ . We therefore only need to show that  $H_b^1(\Sigma)$  is complete. We do this by showing that  $H_{\widehat{b}}^1(\widehat{\Sigma})$  with  $\widehat{b}$  defined as in the proof of Lemma 8 is complete, and proceeding as in Theorem 6. But this is a direct consequence of the fact that  $\widehat{b}$  is a  $A_2$  weight, since this yields that  $\widehat{b}, \widehat{b}^{-1} \in L_{\text{loc}}^1(\mathbb{R}^{d-1})$  and hence that the space  $H_{\widehat{b}}^1(\widehat{\Sigma})$  is a Hilbert space (see, i.e., [22]).  $\square$

**Theorem 15.** *Let  $\Sigma$  be a bounded hypersurface defined by the diffeomorphism  $\alpha : \Sigma \rightarrow \widehat{\Sigma}$  with boundary  $\gamma = \partial\Sigma$ , and let  $b : \Sigma \rightarrow \mathbb{R}$  satisfy Assumptions A1-A4. The space  $C_0^\infty(\widehat{\Sigma}) \cap H_b^1(\Sigma)$  is dense in  $H_b^1(\Sigma)$ .*

*Proof.* We only need to show that  $C_0^\infty(\widehat{\Sigma}) \cap H_b^1(\widehat{\Sigma})$  is dense in  $H_b^1(\widehat{\Sigma})$ . The assertion then follows directly as in the proof of Theorem 6.

Our proof follows [36] (Section 3.2). It is easy to see that for any  $\Psi \in C^k(\widehat{\Sigma})$ ,  $k \in \mathbb{N}$  and  $v \in H_b^1(\widehat{\Sigma})$  we have  $\Psi v \in H_b^1(\widehat{\Sigma})$ . Let  $\eta \in C_0^\infty(\mathbb{R}^{d-1})$  be radial, decreasing and positive with  $\int \eta = 1$ . Define for  $\varepsilon > 0$  a function  $\eta_\varepsilon(x) := \varepsilon^{-d} \eta(x/\varepsilon)$  and  $v_\varepsilon = v * \eta_\varepsilon$ . For all  $v \in L_{b^{\pm 1}}^2(\Sigma)$  we have  $v_\varepsilon \in C_0^\infty(\mathbb{R}^{d-1})$  and  $v_\varepsilon \rightarrow v$  in  $L_{b^{\pm 1}}^2(\widehat{\Sigma})$  [25]. Consequently, for any open  $\widehat{\Sigma}' \Subset \widehat{\Sigma}$  with  $\text{dist}(\widehat{\Sigma}', \widehat{\Sigma}) > 0$  and  $v \in H_b^1(\widehat{\Sigma})$  we have  $v_\varepsilon \rightarrow v$  in  $H_b^1(\widehat{\Sigma}')$  ([36], Lemma 3.3).

We define  $H_{b,0}^1(\widehat{\Sigma})$  as the completion of  $C_0^\infty(\widehat{\Sigma})$ -functions with respect to the  $H_b^1(\widehat{\Sigma})$  norm. Then  $H_{b,0}^1(\widehat{\Sigma})$  is a closed subspace of  $H_b^1(\widehat{\Sigma})$  and therefore a separable Hilbert space. Together with the density property on compact subsets this definition yields that all functions with bounded support in  $H_b^1(\widehat{\Sigma})$  are dense in  $H_b^1(\widehat{\Sigma})$  ([36], Theorem 3.3). With that we can show that the set  $H_b^1(\widehat{\Sigma}) \cap C^\infty(\widehat{\Sigma})$  is dense in  $H_b^1(\widehat{\Sigma})$  ([36], Theorem 3.4 and 3.5).  $\square$

**Theorem 16** (Poincaré–Friedrichs inequality). *Let  $\Sigma$  be a bounded hypersurface defined by the diffeomorphism  $\alpha : \Sigma \rightarrow \widehat{\Sigma}$  with boundary  $\gamma = \partial\Sigma$ , and let  $b : \Sigma \rightarrow \mathbb{R}$  satisfy Assumptions A1-A4. Then there exists a positive constant  $C$  such that for any  $u \in C_0^\infty(\Sigma)$  we have*

$$\|u\|_{0,b^{-1},\Sigma} \leq C \|\nabla_\tau u\|_{0,b,\Sigma}^2.$$

*Proof.* We will show the corresponding result on  $\widehat{\Sigma}$ . A simple coordinate transformation then yields the result. Let  $\widehat{b}$  be defined as in the proof of Lemma 8.

Lemma 4.1 in [10] says that if  $H_{\widehat{b},0}^1(\widehat{\Sigma})$  is compactly embedded in  $L_{\widehat{b}^{-1}}^1(\widehat{\Sigma})$  and if there exist  $x_0 \in \partial\widehat{\Sigma}$  and  $R > 0$  such that  $\widehat{\Sigma}(x_0, R) := B_R(x_0) \cap M$  is a Lipschitz domain and  $\widehat{b}, \widehat{b}^{-1} \in L^1(\Sigma(x_0, R))$ , then the weighted Friedrichs inequality

$$\int_{\widehat{\Sigma}} |v|^{2\widehat{b}^{-1}} \, d\mathbf{s} \leq K \int_{\widehat{\Sigma}} |\nabla v|^{2\widehat{b}} \, d\mathbf{s}$$

holds for all  $v \in C_0^\infty(\widehat{\Sigma})$ . Herein  $\nabla$  denotes the gradient operator on  $\mathbb{R}^{d-1}$ .

It is easy to see that the embedding of  $H_{b,0}^1(\widehat{\Sigma})$  into  $L_{b^{-1}}^1(\widehat{\Sigma})$  is continuous. To show that the embedding is also compact we introduce the space

$$H_{\widehat{bb}}^1(\widehat{\Sigma}) := \left\{ v \in L_b^2(\widehat{\Sigma}) \mid \widehat{\nabla} v \in \mathbf{L}_b^2(\widehat{\Sigma}) \right\},$$

with norm

$$\|v\|_{1,\widehat{bb},\widehat{\Sigma}}^2 := \|v\|_{0,\widehat{b},\widehat{\Sigma}}^2 + \|\nabla v\|_{0,\widehat{b},\widehat{\Sigma}}^2.$$

Again, it is easy to see that this norm is induced by a scalar product. The space  $H_{\widehat{bb}}^1(\widehat{\Sigma})$  equipped with this norm is a Hilbert space [22]. Furthermore, by Theorem 19.11 in [28] it follows that  $H_{\widehat{bb}}^1(\widehat{\Sigma})$  is compactly embedded in  $L_{b^{-1}}^2(\widehat{\Sigma})$ .

Let  $(v_k)_{k \in \mathbb{N}}$  be a bounded sequence in  $H_{b,0}^1(\widehat{\Sigma})$ . Since  $\|v_k\|_{0,\widehat{b},\widehat{\Sigma}}^2 \leq C \|v_k\|_{0,\widehat{b}^{-1},\widehat{\Sigma}}$ , the sequence  $(v_k)_{k \in \mathbb{N}}$  is bounded in  $H_{\widehat{bb}}^1(\widehat{\Sigma})$ . Hence there exists a subsequence  $(v_{k_j})_{j \in \mathbb{N}}$  and a function  $v$  in  $L_{b^{-1}}^2(\widehat{\Sigma})$  with  $s_{k_j} \rightarrow s$  in  $L_{b^{-1}}^2(\widehat{\Sigma})$ . This proves that  $H_b^1(\widehat{\Sigma})$  is compactly embedded in  $L_{b^{-1}}^2(\widehat{\Sigma})$ .

Since  $\widehat{\Sigma}$  is a bounded domain with Lipschitz boundary, its boundary is locally convex, i.e. there exists a neighborhood  $\mathcal{U}$ , where  $\partial\widehat{\Sigma}$  can be represented as convex graph of a Lipschitz continuous function. Take  $x_0 \in \mathcal{U} \cap \partial\widehat{\Sigma}$  and choose  $R$  such that  $B_R(x_0) \subset \mathcal{U}$ , then  $B_R(x_0) \cap \Sigma$  is convex and therefore a Lipschitz domain. By Lemma 8 it follows that  $\widehat{b}$  is an  $A_2$ -weight. This yields  $\widehat{b}, \widehat{b}^{-1} \in L_{\text{loc}}^1(B)$  for all balls  $B$  contained in  $\mathbb{R}^{d-1}$ . Hence we have  $\widehat{b}, \widehat{b}^{-1} \in L_{\text{loc}}^1(B(x_0, R))$ . This proves the assertion, since

$$\begin{aligned} \|v\|_{0,b^{-1},\Sigma} &= \|v \circ \alpha^{-1}\|_{0,\widehat{b}^{-1},\widehat{\Sigma}} \\ &\leq K \|\nabla(v \circ \alpha^{-1})\|_{0,\widehat{b},\Sigma} \\ &= K \|(\nabla_\tau(v) \circ \alpha^{-1}) \nabla \alpha^{-1}\|_{0,\widehat{b},\widehat{\Sigma}} \\ &\leq K \|\nabla \alpha^{-1}\|_{L^\infty(\widehat{\Sigma})} \|\nabla_\tau v\|_{0,b,\Sigma} \\ &= C \|\nabla_\tau v\|_{0,b,\Sigma}. \end{aligned}$$

□

**Remark 17.** We did not prove any trace and extension theorems concerning the space  $H_b^1(\Sigma)$ , but want to mention the following result from [5]. Define the weighted Sobolev space

$$H_{b^{-1}b^{-1}}^1(\Sigma) := \left\{ v \in L_{b^{-1}}^2(\Sigma) \mid \nabla_\tau v \in \mathbf{L}_{b^{-1}}^2(\Sigma) \right\}^2$$

with norm  $\|v\|_{b^{-1}b^{-1},\Sigma}^2 := \|v\|_{0,b^{-1},\Sigma}^2 + \|\nabla_\tau v\|_{0,b^{-1},\Sigma}^2$ . Then  $H_{b^{-1}b^{-1}}^1(\Sigma) \hookrightarrow H_b^1(\Sigma)$ . Furthermore denote by  $H^{\frac{3}{4}}(\gamma)$  the usual Sobolev-Slobodeckij space on  $\gamma$ . Then there exists a linear and continuous trace operator  $\gamma_{b^{-1}} : H_{b^{-1}b^{-1}}^1(\Sigma) \rightarrow H^{\frac{3}{4}}(\gamma)$  and a linear and continuous extension operator  $E_{b^{-1}} : H^{\frac{3}{4}}(\gamma) \rightarrow H_{b^{-1}b^{-1}}^1(\Sigma)$ , such that  $(\gamma_{b^{-1}} \circ E_{b^{-1}}) f = f$  for all  $f \in H^{\frac{3}{4}}(\gamma)$ .

## 4 Weak Formulation

Using the Sobolev spaces introduced in the previous section, we will derive weak formulations of the fluid problem in the bulk, the averaged fluid problem in the fracture and the poroelasticity equation. For fixed crack width functions  $b$  we prove existence and uniqueness of solutions to the coupled fluid–fluid problem. Finally, the weak formulation of the coupled problem is introduced.

### 4.1 Weak Formulations of the Subdomain Problems

We first derive the weak formulation of the three subproblems individually.

#### 4.1.1 The Weak Elastic Problem

Consider the problem defined by the equation (13a) together with boundary conditions (15a), (15b) and (14c). Suppose that  $p^\Omega$  and  $p^\Sigma$  are fixed. Then (13a) is the linear elasticity equation with particular volume terms and boundary conditions. Multiplication of equation (13a) with a test function  $\mathbf{v} \in \mathbf{V}_0$ , integration over  $\Omega$  and the componentwise application of the generalized Green formula (Lemma 3) yields

$$\begin{aligned} \int_{\Omega} \sigma(\mathbf{u}) : \mathbf{e}(\mathbf{v}) \, dx &= (\mathbf{f}_E, \mathbf{v})_{0,\Omega} + (\sigma(\mathbf{u}) \cdot \mathbf{n}, \mathbf{v})_{0,\Gamma_N^E} - (\nabla p^\Omega, \mathbf{v})_{0,\Omega} - (\llbracket \sigma(\mathbf{u}) \rrbracket \cdot \nu, \{\mathbf{v}\})_{0,\Sigma} \\ &\quad - (\{\sigma(\mathbf{u})\} \cdot \nu, \llbracket \mathbf{v} \rrbracket)_{0,\Sigma}. \end{aligned}$$

Inserting the coupling and boundary conditions (14c) and (15a) then yields the equation

$$\int_{\Omega} \sigma(\mathbf{u}) : \mathbf{e}(\mathbf{v}) \, dx = (\mathbf{f}_E, \mathbf{v})_{0,\Omega} + (\sigma_N, \mathbf{v})_{0,\Gamma_N^E} - (\nabla p^\Omega, \mathbf{v})_{0,\Omega} + (p^\Sigma, \{\mathbf{v}\})_{0,\Sigma}.$$

Define the affine space

$$\mathbf{V}_E := \{ \mathbf{u} \in \mathbf{V} \mid \mathbf{u}|_{\Gamma_D^E \setminus \Sigma} = \mathbf{u}_D \}$$

and the bilinear form  $a_E : \mathbf{V}_E \times \mathbf{V}_E \rightarrow \mathbb{R}$  by

$$a_E(\mathbf{u}, \mathbf{v}) := \int_{\Omega} \sigma(\mathbf{u}) : \mathbf{e}(\mathbf{v}) \, dx.$$

Furthermore, introduce the linear forms  $c_{E,p^\Omega} : \mathbf{V}_E \rightarrow \mathbb{R}$  and  $c_{E,p^\Sigma} : \mathbf{V}_E \rightarrow \mathbb{R}$  by

$$c_{E,p^\Omega}(\mathbf{v}) := \int_{\Omega} \nabla p^\Omega \cdot \mathbf{v} \, dx \quad \text{and} \quad c_{E,p^\Sigma}(\mathbf{v}) := \int_{\Sigma} p^\Sigma \llbracket \mathbf{v} \rrbracket \cdot \nu \, da,$$

and  $l_E^\Omega : \mathbf{V}_E \rightarrow \mathbb{R}$  by

$$l_E^\Omega(\mathbf{v}) = \int_{\Omega} \mathbf{f}_E \cdot \mathbf{v} \, dx + \int_{\Gamma_N^E} \sigma_N \cdot \mathbf{v} \, ds.$$

Define  $l_{E,p^\Sigma,p^\Omega} : \mathbf{V}_E \rightarrow \mathbb{R}$  by

$$l_{E,p^\Sigma,p^\Omega}(\mathbf{v}) := l_E^\Omega(\mathbf{v}) - c_{E,p^\Omega}(\mathbf{v}) + c_{E,p^\Sigma}(\mathbf{v}).$$

Then the elasticity problem is formally equivalent to the following weak formulation: For given  $p^\Omega \in V_b$  and  $p^\Sigma \in H_b^1(\Sigma)$ , find  $\mathbf{u} \in \mathbf{V}_E$  such that

$$a_E(\mathbf{u}, \mathbf{v}) = l_{E,p^\Sigma,p^\Omega}(\mathbf{v}) \quad \forall \mathbf{v} \in \mathbf{V}_0. \quad (16)$$

This problem is a standard linear elasticity problem in fractured domains. It has a unique solution, which depends continuously on the data  $p^\Omega$  and  $p^\Sigma$  from the fluid problems. A proof can be found in [20].

**Theorem 18.** *Let  $\Sigma$  be of class  $C^2$ , and suppose that  $\mu \geq 0$  and  $\lambda + 2\mu \geq 0$ . Assume that the Dirichlet boundary  $\Gamma_D^E$  has a positive  $(d-1)$ -dimensional measure. Let  $p^\Sigma \in H_b^1(\Sigma)$  and  $p^\Omega \in V_b$ , and assume that  $\mathbf{u}_D = \mathbf{0}$  and  $\sigma_N = \mathbf{0}$ . Then there exists a unique solution  $\mathbf{u} \in \mathbf{V}_E$  to problem (16). Furthermore the estimate*

$$\|\mathbf{u}\|_{\mathbf{V}_E} \leq \frac{C}{2\mu} \left( \|\mathbf{f}_E\|_{0,\Omega} + \|\nabla p^\Omega\|_{0,\Omega} + \|p^\Sigma\|_{0,\Sigma} \right)$$

is satisfied for a constant  $C$  depending only on the domain  $\Omega$ .

We now want to gain a better understanding of the behavior of the solution near the crack tip. It is well known in the literature that the weak solution of a linear elastic problem in a fractured domain can be decomposed into a singular term  $\mathbf{u}_s$  and a regular term  $\mathbf{u}_r$ , where the singular term describes the discontinuous behavior of the solution across the fracture and the singular behavior of the stress nearby the crack front [21, 6]. To understand the behavior of the solution near a single the crack front we introduce a polar coordinate frame  $(r, \Theta)$  with  $\Theta = 0$  along the tangential extension of the fracture and  $r := \text{dist}(\mathbf{x}, \gamma)$  for all  $x \in \mathbb{R}^d$ . In three dimensions we extend this frame to a cylindrical coordinate frame by introducing a parametrization of  $\gamma$  and using the arc length parameter as third coordinate.

Rewriting equations (13a), (14c) in polar or cylindrical coordinates, and applying the Mellin transform

$$\widehat{u}(\alpha; \Theta) := \mathcal{M}[u(r, \Theta)](\alpha) = \int_{\mathbb{R}^+} r^{-\alpha-1} u(r, \Theta) \, dr$$

to the resulting problem, generates a differential equation with parameter  $\alpha \in \mathbb{C}$ . All  $\alpha$  for which the resulting problem with zero right-hand-side admits nontrivial solutions  $\mathbf{v}_\alpha(\Theta)$  are called eigenvalues, and the corresponding functions  $\mathbf{v}_\alpha(\Theta)$  are called eigenvectors. These eigenvectors determine the singularity of the problem.

**Theorem 19.** *Let  $\Omega \subset \mathbb{R}^2$  or  $\Omega \subset \mathbb{R}^3$ .*

- (i) *The eigenvalues of the elasticity problem with symmetric Neumann boundary conditions on the fracture are given by  $\Lambda_E = \{k/2 \mid k \in \mathbb{Z}\}$ .*
- (ii) *The Mellin transform is well defined and invertible for all  $\alpha$  with  $\text{Re}(\alpha) \notin \Lambda_E$ . Hence  $\widehat{u}(\alpha, \Theta)$  is holomorphic for all  $\alpha$  with  $\text{Re}(\alpha) \in \mathbb{R} \setminus \Lambda_E$ .*
- (iii) *The singular part  $\mathbf{u}_s$  of the solution to the elasticity problem with symmetric Neumann boundary conditions on the fracture is of the form*

$$\mathbf{u}_s = \chi \left( K_{\frac{1}{2}}^{(1)} \mathbf{v}_{\frac{1}{2}}^{(1)} + K_{\frac{1}{2}}^{(2)} \mathbf{v}_{\frac{1}{2}}^{(2)} + K_{\frac{1}{2}}^{(3)} \mathbf{v}_{\frac{1}{2}}^{(3)} \right)$$

*near the crack front. The real constants  $K_{\frac{1}{2}}^{(i)}$  are called stress intensity factors and  $\chi$  is a smooth cutoff-function, which is equal to one in a neighborhood of the crack front. The components of the eigenfunctions  $\mathbf{v}_{\frac{1}{2}}^{(i)}$  are in the span of the set*

$$\widetilde{\mathcal{S}} = \{ \sin(\Theta/2), \cos(\Theta/2), \sin(\Theta) \sin(\Theta/2), \sin(\Theta) \cos(\Theta/2) \}.$$

The important conclusion from the latter Theorem is, that the fracture width function  $b$  can be approximated nearby the crack tip by

$$b = \llbracket \mathbf{u}_s \rrbracket \cdot \nu \simeq r^{\frac{1}{2}} = \text{dist}(\cdot, \gamma)^{\frac{1}{2}}.$$

We want to mention, that we only considered edge asymptotics in the three-dimensional case here, since  $\Sigma$  is smooth enough. If  $\Sigma$  only has a Lipschitz boundary, then vertex singularities have to be considered as well.

#### 4.1.2 The Fluid Bulk Problem

Assume next that the width  $b \in H_{00}^{\frac{1}{2}}(\Sigma)$  and the fracture fluid pressure  $p^\Sigma \in H_b^1(\Sigma)$  are fixed. We consider the fluid bulk problem introduced by the equations (13b), (13c) together with the boundary conditions (15c), (15d) and the coupling conditions (14a), (14b) and (14d). Let

$$V_F^\Omega := \left\{ p^\Omega \in V_b \mid p^\Omega|_{\Gamma_E \setminus \widetilde{\Sigma}} = p_D^\Omega \right\} \quad \text{and} \quad V_{b,0} = \left\{ r^\Omega \in V_b \mid r^\Omega|_{\Gamma_E \setminus \widetilde{\Sigma}} = 0 \right\}.$$

We multiply equation (13b) with a test function and apply the generalized Green's formula (see Lemma 3) to derive the equation

$$(f_F^\Omega, r^\Omega)_{0,\Omega} - (\mathbf{q}^\Omega \cdot \mathbf{n}, r^\Omega)_{0,\Gamma_N^F} = -(\mathbf{q}^\Omega, \nabla r^\Omega)_{0,\Omega} - (\llbracket \mathbf{q}^\Omega \rrbracket \cdot \nu, \{r^\Omega\})_{0,\Sigma} - (\{\mathbf{q}^\Omega\} \cdot \nu, \llbracket r^\Omega \rrbracket)_{0,\Sigma}.$$

Replacing the bulk fluid velocity jump  $\llbracket \mathbf{q}^\Omega \rrbracket \cdot \nu$  and average  $\{\mathbf{q}^\Omega\} \cdot \nu$  by the corresponding pressure values in the coupling conditions (14a) and (14b) yields the equation

$$(f_F^\Omega, r^\Omega)_{0,\Omega} - (\mathbf{q}^\Omega \cdot \mathbf{n}, r^\Omega)_{0,\Gamma_N^F} = -(\mathbf{q}^\Omega, \nabla r^\Omega)_{0,\Omega} - \frac{1}{2\xi - 1} \left( \frac{4K^\nu}{b} (p^\Sigma - \{p^\Omega\}), \{r^\Omega\} \right)_{0,\Sigma} + \left( \frac{K^\nu}{b} \llbracket p^\Omega \rrbracket, \llbracket r^\Omega \rrbracket \right)_{0,\Sigma}.$$

Inserting the momentum equation (13c) and the Neumann boundary conditions (15c), we derive the weak problem: For given  $b \in H_{00}^{\frac{1}{2}}(\Sigma)$  and  $p^\Sigma \in H_b^1(\Sigma)$ , find  $p^\Omega \in V_F^\Omega$  such that

$$a_{F,b}^\Omega(p^\Omega, r^\Omega) - c_{F,b,p^\Sigma}(r^\Omega) = l_F^\Omega(r^\Omega) \quad \forall r^\Omega \in V_{b,0}^\Omega. \quad (17)$$

Here, the bilinear form  $a_F^\Omega : V_F^\Omega \times V_F^\Omega \rightarrow \mathbb{R}$  is defined by

$$a_{F,b}^\Omega(p^\Omega, r^\Omega) := (\mathbb{K} \nabla p^\Omega, \nabla r^\Omega)_{0,\Omega} + \frac{1}{2\xi - 1} \left( \frac{4K^\nu}{b} \{p^\Omega\}, \{r^\Omega\} \right)_{0,\Sigma} + \left( \frac{K^\nu}{b} \llbracket p^\Omega \rrbracket, \llbracket r^\Omega \rrbracket \right)_{0,\Sigma}.$$

The linear form  $c_{F,b,p^\Sigma} : V_F^\Omega \rightarrow \mathbb{R}$ ,

$$c_{F,b,p^\Sigma}(r^\Omega) := \frac{1}{2\xi - 1} \left( \frac{4K^\nu}{b} p^\Sigma, \{r^\Omega\} \right)_{0,\Sigma}$$

represents the coupling to the fracture fluid pressure  $p^\Sigma$ . Finally, the linear form  $l_F^\Omega : V_F^\Omega \rightarrow \mathbb{R}$

$$l_F^\Omega(r^\Omega) := (f_F^\Omega, r^\Omega)_{0,\Omega} - (q_N^\Omega, r^\Omega)_{0,\Gamma_N^F},$$

represents the external source terms.

The map  $a_{F,b}^\Omega$  is symmetric and bilinear in  $p^\Omega$  and  $r^\Omega$ , but depends nonlinearly on the fracture width  $b = \llbracket \mathbf{u} \rrbracket \cdot \nu$ . Consequently, it depends nonlinearly on the displacement field  $\mathbf{u}$ . We postpone the discussion on the existence of weak solutions to Section 4.2.

#### 4.1.3 Fracture Fluid Problem

Suppose now that the fracture width  $b \in H_{00}^{\frac{1}{2}}(\Sigma)$  and the bulk fluid pressure  $p^\Omega \in V_F^\Omega$  are fixed. Define

$$V_F^\Sigma := \left\{ p^\Sigma \in H_b^1(\Sigma) \mid p^\Sigma|_{\gamma_D^F} = p_D^\Sigma \right\} \quad \text{and} \quad H_{b,0}^1(\Sigma) := \left\{ r^\Sigma \in H_b^1(\Sigma) \mid r^\Sigma|_{\gamma_D^F} = 0 \right\}.$$

Consider the averaged fluid problem on the fracture, given by Equations (13d) and (13e), together with the boundary conditions (15e), and (15f) and the coupling conditions (14d) and (14a). Insert (13e) into (13d), and multiply it with a test function  $r^\Sigma \in V_F^\Sigma$ . We integrate the resulting Laplace–Beltrami-like problem over  $\Sigma$  and apply integration by parts, to obtain

$$(bK^\tau \nabla p^\Sigma, \nabla r^\Sigma)_{0,\Sigma} = (bf^\Sigma, r^\Sigma)_{0,\Sigma} - (\llbracket \mathbf{q}^\Omega \rrbracket \cdot \nu, r^\Sigma)_{0,\Sigma} - (\kappa b \{\mathbf{q}^\Omega\} \cdot \nu, r^\Sigma)_{0,\Sigma} - (bq_N^\Sigma, r^\Sigma)_{0,\gamma_N^F}.$$

Using equation (14a) to replace the fluid velocity normal jump by a term only depending on  $p^\Sigma$  and  $p^\Omega$  yields the following problem: For given  $b \in H_{00}^{\frac{1}{2}}(\Sigma)$  and  $p^\Omega \in V_F^\Omega$ , find  $p^\Sigma \in V_F^\Sigma$ , such that

$$a_{F,b}^\Sigma(p^\Sigma, r^\Sigma) - c_{F,b,p^\Omega}(r^\Sigma) = l_{F,b}^\Sigma(r^\Sigma) \quad \forall r^\Sigma \in H_{b,0}^1(\Sigma). \quad (18)$$

Here, the bilinear form  $a_{F,b}^\Sigma : V_F^\Sigma \times V_F^\Sigma$  is defined by

$$a_{F,b}^\Sigma(p^\Sigma, r^\Sigma) := (bK^\tau \nabla_\tau p^\Sigma, \nabla_\tau r^\Sigma)_\Sigma + \frac{1}{2\xi - 1} \left( \frac{4K^\nu}{b} p^\Sigma, r^\Sigma \right)_{0,\Sigma},$$

the linear form  $c_{F,b,p^\Omega} : V_F^\Sigma \rightarrow \mathbb{R}$  by

$$c_{F,b,p^\Omega}(r^\Sigma) := \frac{1}{2\xi - 1} \left( \frac{4K^\nu}{b} r^\Sigma, \{p^\Omega\} \right)_{0,\Sigma} + (\kappa K^\nu \llbracket p^\Omega \rrbracket, r^\Sigma)_{0,\Sigma},$$

and the source term  $l_F^\Sigma : \mathbf{V}_F^\Sigma \rightarrow \mathbb{R}$  is defined by

$$l_{F,b}^\Sigma(r^\Sigma) = (bf^\Sigma, r^\Sigma)_{0,\Sigma} - (bq_N^\Sigma, r^\Sigma)_{0,\gamma_N^\Sigma}.$$

The map  $a_{F,b}^\Sigma$  is symmetric and bilinear in  $p^\Sigma$  and  $r^\Sigma$ , but depends nonlinearly on  $\mathbf{u}$  through the fracture width  $b = \llbracket \mathbf{u} \rrbracket \cdot \nu$ . The map  $l_{F,b}^\Sigma$  is linear in  $r^\Sigma$ , but also depends linearly on  $\mathbf{u}$ . Note that the curvature  $\kappa$  only plays a role if  $p^\Omega$  does jump across the fracture. Existence and uniqueness of solutions to this problem is discussed in the next section.

## 4.2 Existence of Solutions of the Weak Fluid–Fluid Problem

For a fixed crack width function  $b$ , the coupled fluid problems (17) and (18) form a joint linear variational problem. From the asymptotic expansion of the displacement field  $\mathbf{u}$  (Section 4.1.1) we know that  $b$  behaves like  $\text{dist}^{\frac{1}{2}}(\cdot, \gamma)$  near the crack tip. This allows us to show existence of unique solutions to the coupled fluid–fluid problem in suitable weighted Sobolev spaces, under the assumption that the crack is open.

To this end, we define the bilinear forms  $c_{F,b} : V_F^\Sigma \times V_F^\Omega \rightarrow \mathbb{R}$  by

$$c_{F,b}(r^\Sigma, r^\Omega) := c_{F,b,r^\Sigma}(r^\Omega) = c_{F,b,r^\Sigma}(r^\Sigma) - (\kappa K^\nu \llbracket r^\Omega \rrbracket, r^\Sigma)_{0,\Sigma}$$

and  $c_{F,b,\kappa} : V_F^\Sigma \times V_F^\Omega \rightarrow \mathbb{R}$  by

$$c_{F,\kappa}(r^\Sigma, r^\Omega) := (\kappa K^\nu \llbracket r^\Omega \rrbracket, r^\Sigma)_{0,\Sigma}.$$

For given  $b \in H_{00}^{\frac{1}{2}}(\Sigma)$  combining the weak formulations (17) and (18) yields: find  $p^\Sigma \in V_F^\Sigma$  and  $p^\Omega \in V_F^\Omega$  such that

$$a_{F,b}^\Omega(p^\Omega, r^\Omega) - c_{F,b}(p^\Sigma, r^\Omega) = l_F^\Omega(r^\Omega) \quad \forall r^\Omega \in V_{b,0}, \quad (19a)$$

$$a_{F,b}^\Sigma(p^\Sigma, r^\Sigma) - c_{F,b}(r^\Sigma, p^\Omega) - c_{F,b,\kappa}(r^\Sigma, p^\Omega) = l_{F,b}^\Sigma(r^\Sigma) \quad \forall r^\Sigma \in H_{b,0}^1(\Sigma). \quad (19b)$$

We now prove existence and uniqueness of a solution of this weak coupled fluid–fluid problem.

**Theorem 20.** *Assume that  $|\kappa| \leq \kappa_{max} < \infty$  and that  $\mathbb{K}$  is symmetric, bounded and uniformly elliptic, i.e., there exists a constant  $K > 0$  such that*

$$x^T \mathbb{K} x > K \|x\|^2 \quad \forall x \in \mathbb{R}^d \quad \text{and} \quad \text{a.e. on } \Omega.$$

*Furthermore, assume that  $K^\tau, K^\nu$  are positive constants. Let  $b$  satisfy Assumptions 7 and let  $\xi \in (\frac{1}{2}, 1]$ . Suppose that the curvature of the fracture is bounded in the sense that*

$$b_{max}^2 \kappa_{max}^2 < \frac{4K^\tau}{K^\nu} C_\Sigma,$$

*where  $C_\Sigma$  denotes the Poincaré constant of  $\Sigma$  from Theorem 16. Let  $\Gamma_D^F \neq \emptyset$ ,  $f_F^\Omega \in L^2(\Omega)$ ,  $f_F^\Sigma \in L_+^2(\Sigma)$ ,  $q_N^\Omega \in L^2(\Gamma_N)$ , and  $q_N^\Sigma \in L_+^2(\Sigma)$ . Finally, assume that*

$$p_D^\Omega \in W_D^\Omega := \left\{ s \in H^{\frac{1}{2}}(\Gamma_D^F) \mid E_\Omega s \in V_b \right\}, \quad p_D^\Sigma \in W_D^\Sigma := \left\{ s \in H^{\frac{1}{2}}(\gamma_D^F) \mid E_\Sigma s \in H_b^1(\Sigma) \right\},$$

*where  $E_\Omega : H^{\frac{1}{2}}(\Gamma_D^F) \rightarrow V$  and  $E_\Sigma : H^{\frac{1}{2}}(\gamma_D^F) \rightarrow H^1(\Sigma)$  are the standard extension operators. Then there exists a unique solution  $(p^\Sigma, p^\Omega) \in V_F^\Sigma \times V_F^\Omega$  of the weak coupled problem (19).*

Before presenting the proof, note first that the trace space  $W_D^\Omega$  is not empty. From the trace theorem 11 we know that the trace of a  $V_b$ -function restricted to  $\Gamma_D^F$  is in  $H^{\frac{1}{2}}(\Gamma_D^F)$ . By Lemma 12 we conclude that the trace of this  $V_b$ -function restricted to  $\Sigma$  is in  $W_b$ . And thus, again by Lemma 12, it follows that the application of the global extension operator yields the identity and thus a  $V_b$ -function.

Similarly, the space  $W_D^\Sigma$  is not empty. By Remark 17 each function in  $H^{\frac{3}{4}}(\gamma_D)$  has an extension in  $H_{-b,-b}^1(\Sigma)$  and thus in  $H_b^1(\Sigma)$ .

*Proof.* Without loss of generality we assume that  $p_D^\Omega = 0$  and  $p_D^\Sigma = 0$ . Then  $V_F := V_F^\Sigma \times V_F^\Omega = H_{b,0}^1(\Sigma) \times V_{b,0}$ , and we equip this space with the norm  $\|(p^\Sigma, p^\Omega)\|_{V_F}^2 := \|p^\Sigma\|_{1,b,\Sigma}^2 + \|p^\Omega\|_{1,b^{-1},\Omega}^2$ . Define the bilinear form  $k_b : V_F \times V_F \rightarrow \mathbb{R}$  by adding the left hand sides of (19a) and (19b)

$$k_b(p, r) := a_{F,b}^\Omega(p^\Omega, r^\Omega) + a_{F,b}^\Sigma(p^\Sigma, r^\Sigma) - c_{F,b}(p^\Sigma, r^\Omega) - c_{F,b}(r^\Sigma, p^\Omega) - c_{F,b,\kappa}(r^\Sigma, p^\Omega).$$

Likewise, define the linear form  $l_b : V_F \rightarrow \mathbb{R}$  by adding the right hand sides of (19a) and (19b)

$$l_b(r) = l_F^\Omega(r^\Omega) + l_{F,b}^\Sigma(r^\Sigma),$$

where  $p = (p^\Sigma, p^\Omega) \in V_F$  and  $r = (r^\Sigma, r^\Omega) \in V_F$ . It is easy to check that each solution  $p \in V_F$  of the problem

$$k_b(p, r) = l(r) \quad \forall r \in V_F \quad (20)$$

is a weak solution of problem (19) and vice versa.

We will now prove existence and uniqueness of a solution to (20) using the Lax–Milgram Lemma. The continuity of the linear form  $l$  can be easily shown using the Cauchy–Schwarz inequality. Similarly, boundedness of the bilinear form  $k_b$  can be shown using the Cauchy–Schwarz inequality, the boundedness of the permeability tensors, and the continuity of the trace operators.

To prove that  $k$  is coercive, we introduce the map  $g_b : V_F \rightarrow \mathbb{R}$

$$g_b(p) := \frac{4}{2\xi - 1} \left[ (K^\nu b^{-1} \{p^\Omega\}, \{p^\Omega\})_{0,\Sigma} + (K^\nu b^{-1} p^\Sigma, p^\Sigma)_{0,\Sigma} - 2 (K^\nu b^{-1} p^\Sigma, \{p^\Omega\})_{0,\Sigma} \right] \\ + (K^\nu b^{-1} \llbracket p^\Omega \rrbracket, \llbracket p^\Omega \rrbracket)_{0,\Sigma} - (\kappa K^\nu \llbracket p^\Omega \rrbracket, p^\Sigma)_{0,\Sigma},$$

and we note that

$$g_b(p) = k_b(p, p) - (\mathbb{K} \nabla p^\Omega, \nabla p^\Omega)_{0,\Omega} - (b K^\tau \nabla_\tau p^\Sigma, \nabla_\tau p^\Sigma)_{0,\Sigma}.$$

From the Cauchy–Schwarz inequality and the  $\varepsilon$ -weighted Young inequality

$$|ab| = |\varepsilon^{\frac{1}{2}} a| |\varepsilon^{-\frac{1}{2}} b| \leq \frac{1}{2} (\varepsilon a^2 + \varepsilon^{-1} b^2) \quad \forall a, b \in \mathbb{R}, \quad \varepsilon > 0,$$

we deduce that for any  $\varepsilon_1 > 0$

$$(b^{-1} K^\nu p^\Sigma, \{p^\Omega\})_{0,\Sigma} \leq K^\nu \|p^\Sigma\|_{0,b^{-1},\Sigma} K^\nu \|\{p^\Omega\}\|_{0,b^{-1},\Sigma} \\ \leq \frac{1}{2} \left( \varepsilon_1 K^\nu \|p^\Sigma\|_{0,b^{-1},\Sigma}^2 + \frac{K^\nu}{\varepsilon_1} \|\{p^\Omega\}\|_{0,b^{-1},\Sigma}^2 \right),$$

and that for any  $\varepsilon_2 > 0$

$$(\kappa K^\nu \llbracket p^\Omega \rrbracket, p^\Sigma)_{0,\Sigma} \leq K^\nu b_{\max} \kappa_{\max} \left( \frac{1}{b} \llbracket p^\Omega \rrbracket, p^\Sigma \right)_{0,\Sigma} \\ \leq \frac{1}{2} \left( \varepsilon_2 K^\nu b_{\max} \kappa_{\max} \|\llbracket p^\Omega \rrbracket\|_{0,b^{-1},\Sigma}^2 + \frac{K^\nu b_{\max} \kappa_{\max}}{\varepsilon_2} \|p^\Sigma\|_{0,b^{-1},\Sigma}^2 \right).$$

Using these inequalities we can find a lower bound for  $g_b(p)$

$$\begin{aligned}
g_b(p) &= \frac{4K^\nu}{2\xi - 1} \left[ \|\{p^\Omega\}\|_{0,b^{-1},\Sigma}^2 + \|p^\Sigma\|_{0,b^{-1},\Sigma}^2 - 2(b^{-1}p^\Sigma, \{p^\Omega\})_{0,\Sigma} \right] \\
&\quad + K^\nu \|\llbracket p^\Omega \rrbracket\|_{0,b^{-1},\Sigma}^2 - (\kappa K^\nu \llbracket p^\Omega \rrbracket, p^\Sigma)_{0,\Sigma} \\
&\geq \frac{4K^\nu}{2\xi - 1} \left[ (1 - \varepsilon_1) \|\{p^\Omega\}\|_{0,b^{-1},\Sigma}^2 + \frac{\varepsilon_1 - 1}{\varepsilon_1} \|p^\Sigma\|_{0,b^{-1},\Sigma}^2 \right] \\
&\quad + \frac{2 - b_{\max} \kappa_{\max} \varepsilon_2}{2} K^\nu \|\llbracket p^\Omega \rrbracket\|_{0,b^{-1},\Sigma}^2 - \frac{b_{\max} \kappa_{\max}}{2\varepsilon_2} K^\nu \|p^\Sigma\|_{0,b^{-1},\Sigma}^2 \\
&= \frac{4K^\nu(1 - \varepsilon_1)}{2\xi - 1} \|\{p^\Omega\}\|_{0,b^{-1},\Sigma}^2 + \frac{2 - b_{\max} \kappa_{\max} \varepsilon_2}{2} K^\nu \|\llbracket p^\Omega \rrbracket\|_{0,b^{-1},\Sigma}^2 \\
&\quad + \frac{(8\varepsilon_1 - 8)\varepsilon_2 - b_{\max} \kappa_{\max} (2\xi - 1)\varepsilon_1}{2\varepsilon_1 \varepsilon_2 (2\xi - 1)} K^\nu \|p^\Sigma\|_{0,b^{-1},\Sigma}^2.
\end{aligned}$$

We use this result to find a lower bound for  $k_b(p, p)$ . Introducing the constant  $\eta \in (0, 1)$ , we have

$$\begin{aligned}
k_b(p, p) &= \|\mathbb{K}^{\frac{1}{2}} \nabla p^\Omega\|_{0,\Omega}^2 + \|(K^\tau)^{\frac{1}{2}} \nabla_\tau p^\Sigma\|_{0,b,\Sigma}^2 + g_b(p) \\
&\geq K \|\nabla p^\Omega\|_{0,\Omega}^2 + K^\tau \|\nabla_\tau p^\Sigma\|_{0,b,\Sigma}^2 + g_b(p) \\
&\geq \frac{K}{2} \min\{1, C_\Omega\} \|p^\Omega\|_{1,\Omega}^2 + \eta K^\tau C_\Sigma \|p^\Sigma\|_{0,b^{-1},\Sigma}^2 + (1 - \eta) K^\tau \|\nabla_\tau p^\Sigma\|_{0,b,\Sigma}^2 + g_b(p) \\
&\geq \frac{K}{2} \min\{1, C_\Omega\} \|p^\Omega\|_{1,\Omega}^2 + \eta K^\tau C_\Sigma \|p^\Sigma\|_{0,b^{-1},\Sigma}^2 + (1 - \eta) K^\tau \|\nabla_\tau p^\Sigma\|_{0,b,\Sigma}^2 \\
&\quad + \frac{4K^\nu(1 - \varepsilon_1)}{2\xi - 1} \|\{p^\Omega\}\|_{0,b^{-1},\Sigma}^2 + \frac{2 - b_{\max} \kappa_{\max} \varepsilon_2}{2} K^\nu \|\llbracket p^\Omega \rrbracket\|_{0,b^{-1},\Sigma}^2 \\
&\quad + \frac{(8\varepsilon_1 - 8)\varepsilon_2 - b_{\max} \kappa_{\max} (2\xi - 1)\varepsilon_1}{2\varepsilon_1 \varepsilon_2} K^\nu \|p^\Sigma\|_{0,b^{-1},\Sigma}^2 \\
&= \frac{K}{2} \min\{1, C_\Omega\} \|p^\Omega\|_{1,\Omega}^2 + (1 - \eta) K^\tau \|\nabla_\tau p^\Sigma\|_{0,b,\Sigma}^2 \\
&\quad + \frac{4K^\nu(1 - \varepsilon_1)}{2\xi - 1} \|\{p^\Omega\}\|_{0,b^{-1},\Sigma}^2 + \frac{2 - b_{\max} \kappa_{\max} \varepsilon_2}{2} K^\nu \|\llbracket p^\Omega \rrbracket\|_{0,b^{-1},\Sigma}^2 \\
&\quad + \frac{[(2\eta K^\tau C_\Sigma (2\xi - 1) + 8K^\nu)\varepsilon_1 - 8K^\nu]\varepsilon_2 - b_{\max} \kappa_{\max} (2\xi - 1) K^\nu \varepsilon_1}{2\varepsilon_1 \varepsilon_2 (2\xi - 1)} \|p^\Sigma\|_{0,b^{-1},\Sigma}^2,
\end{aligned}$$

where we have used the Poincaré inequalities on  $\Sigma$  and  $\Omega$  with positive constants  $C_\Sigma$  and  $C_\Omega$ .

To ensure coercitivity all coefficients in the last estimate need to be positive. We therefore have to find constants  $\varepsilon_1 \in (0, 1)$ ,  $\varepsilon_2 \in \left(0, \frac{2}{b_{\max} \kappa_{\max}}\right)$ , and  $\eta \in (0, 1)$ , such that

$$\frac{[(2\eta K^\tau C_\Sigma (2\xi - 1) + 8K^\nu)\varepsilon_1 - 8K^\nu]\varepsilon_2 - b_{\max} \kappa_{\max} (2\xi - 1) K^\nu \varepsilon_1}{2\varepsilon_1 \varepsilon_2 (2\xi - 1)} \geq 0.$$

This inequality holds if and only if

$$[(2\eta K^\tau C_\Sigma (2\xi - 1) + 8K^\nu)\varepsilon_1 - 8K^\nu]\varepsilon_2 \geq b_{\max} \kappa_{\max} (2\xi - 1) K^\nu \varepsilon_1. \quad (21)$$

Since  $b_{\max}^2 \kappa_{\max}^2 < \frac{4K^\tau C_\Sigma}{K^\nu}$  by assumption, we have  $0 \leq \frac{b_{\max}^2 \kappa_{\max}^2 K^\nu}{4K^\tau C_\Sigma} < 1$ . Hence choose any  $\eta > \frac{b_{\max}^2 \kappa_{\max}^2 K^\nu}{4K^\tau C_\Sigma}$  less than one. This yields  $4K^\tau C_\Sigma \eta - b_{\max}^2 \kappa_{\max}^2 K^\nu > 0$  and thus

$$0 < C_1 := \frac{16K^\nu}{[4K^\tau C_\Sigma \eta - b_{\max}^2 \kappa_{\max}^2 K^\nu](2\xi - 1) + 16K^\nu} < 1.$$

Now choose  $\varepsilon_1 > C_1$ . Then we have

$$\begin{aligned} 2[(2K^\tau C_\Sigma \eta (2\xi - 1) + 8K^\nu) \varepsilon_1 - 8K^\nu] &= (4K^\tau C_\Sigma \eta (2\xi - 1) + 16K^\nu) \varepsilon_1 - 16K^\nu \\ &> b_{\max}^2 \kappa_{\max}^2 K^\nu (2\xi - 1) \varepsilon_1, \end{aligned}$$

or equivalently

$$\frac{2}{b_{\max} \kappa_{\max}} > C_2 := \frac{b_{\max} \kappa_{\max} K^\nu (2\xi - 1) \varepsilon_1}{(2\eta K^\tau C_\Sigma (2\xi - 1) + 8K^\nu) \varepsilon_1 - 8K^\nu} \geq 0.$$

Finally, choose  $\varepsilon_2 > C_2$ . Then estimate (21) is satisfied.

This choice for  $\varepsilon_1$ ,  $\varepsilon_2$  and  $\eta$ , implies that there exists a positive constant  $C$ , which only depends on  $\Omega$ ,  $\Sigma$ ,  $K^\nu$ ,  $K^\tau$ ,  $K$ ,  $\xi$ ,  $\varepsilon_1$ ,  $\varepsilon_2$  and  $\eta$ , such that

$$k_b(p, p) \geq C \|p\|_{V_F}^2.$$

Hence  $k_b$  is coercive on  $V_F$ , and from the Lax–Milgram Lemma follows that (20) has a unique solution in  $V_F$ , which in turn implies the original assertion.  $\square$

**Remark 21.** *Asymptotic analysis for the bulk fluid problem with fixed  $p^\Sigma$ , as it was done for the elasticity problem in Section 4.1.1, is difficult due to the  $b$ -dependent and non-symmetric coupling conditions on  $\Sigma$ . It is not clear to the authors whether these coupling conditions can be addressed by the standard spectral theory for elliptic problems with variable coefficients. Nonetheless, the primal form of the bulk fluid problem is a simple Laplace-type problem. The asymptotic expansion of this problem for various types of boundary conditions is well known [21]. Eigenfunctions are of the form  $c_1 r^\alpha \sin(\alpha\Theta) + c_2 r^\alpha \cos(\alpha)$ , and for plane problems with Neumann or Dirichlet boundary conditions on  $\Sigma$  we have that  $\alpha = 1/2$  is the lowest order term of the asymptotic expansion.*

### 4.3 The Coupled Weak Problem

Combining the three individual problems and coupling terms we obtain the coupled weak problem: Find  $(\mathbf{u}, p^\Omega, p^\Sigma) \in \mathbf{V}_E \times V_F^\Omega \times V_F^\Sigma$  such that

$$a_F^\Omega(\mathbf{u}, p^\Omega, r^\Omega) - c_F(\mathbf{u}, p^\Sigma, r^\Omega) = l_F^\Omega(r^\Omega) \quad \forall r^\Omega \in V_{b,0}, \quad (22a)$$

$$a_F^\Sigma(\mathbf{u}, p^\Sigma, r^\Sigma) - c_F(\mathbf{u}, r^\Sigma, p^\Omega) - c_{F,\kappa}(\mathbf{u}, r^\Sigma, p^\Omega) = l_F^\Sigma(\mathbf{u}, r^\Sigma) \quad \forall r^\Sigma \in H_{b,0}^1(\Sigma), \quad (22b)$$

$$a_E(\mathbf{u}, \mathbf{v}) - c_E^\Omega(\mathbf{v}, p^\Omega) + c_E^\Sigma(\mathbf{v}, p^\Sigma) = l_E^\Omega(\mathbf{v}) \quad \forall \mathbf{v} \in \mathbf{V}_0. \quad (22c)$$

All terms in these three equations are as defined in the previous sections, with the only difference that the dependencies on  $b = \llbracket \mathbf{u} \rrbracket \cdot \nu$  are replaced by dependencies on  $\mathbf{u}$ .

The complete problem (22) is nonlinear through the intricate influence of the changing crack width  $b$  on the fluid flow in the fracture. Attempting to solve the entire system monolithically using a Newton-type method is certainly an option. However, as both the fluid–fluid problem and the elasticity problem are linear when regarded separately, it is much more convenient to use a substructuring solver that iterates between the two. As the numerical tests in Section 6 show, such a substructuring solver converges in very few iterations.

We therefore proceed to write the coupled system as a fixed-point equation. Since the fluid problems depend on the displacement only through the crack width  $b = \llbracket \mathbf{u} \rrbracket \cdot \nu$ , we write the fixed-point equation in this variable. By Theorem 20, the coupled fluid–fluid problem (19) has a unique solution  $(p^\Sigma, p^\Omega) \in V_F^\Sigma \times V_F^\Omega$  for any  $b \in H_{00}^{1/2}(\Sigma)$  satisfying Assumptions 7. We therefore obtain that the fluid solution operator

$$S_f : b \mapsto (p^\Omega, p^\Sigma)$$

is well-defined. Showing continuity of this operator is problematic, as the spaces  $V_F^\Sigma$  and  $V_F^\Omega$  depend on the argument  $b$ .

Likewise, by Theorem 18, the elasticity problem (16) has a unique solution for each  $(p^\Omega, p^\Sigma) \in V_F^\Sigma \times V_F^\Omega$ . Consequently, the elasticity solution operator

$$S_e : (p^\Omega, p^\Sigma) \mapsto \mathbf{u}$$

is well-defined, and Theorem 18 additionally shows that it is even continuous.

Finally, the normal jump operator

$$j : \mathbf{V}_E \rightarrow H_{00}^{1/2}(\Sigma), \quad j : \mathbf{u} \mapsto b := \llbracket \mathbf{u} \rrbracket \cdot \nu$$

is well-defined and continuous. Hence, we can write the weak coupled system as the fixed-point problem: Find  $b \in H_{00}^{1/2}(\Sigma)$  satisfying Assumptions 7 such that

$$b = (j \circ S_e \circ S_f)b. \quad (23)$$

Showing existence of solutions to this equation is beyond the scope of this work.

## 5 Discretization and Solver

For the discretization of the coupled problem (22) we use two unrelated grids: A  $d$ -dimensional one for the bulk fluid and elasticity problems, and a  $(d-1)$ -dimensional one for the fracture fluid equation. We use first-order Lagrange finite elements for the fluid equation on the fracture. Discretizing the bulk equations is more challenging: Both solution fields are discontinuous at the fracture, and both fields develop singularities at fracture tips. These problems are overcome by an appropriate XFEM discretization.

### 5.1 Finite Element Discretization of the Fracture Flow Equation

Denote by  $\mathcal{S}_h$  a conforming and shape regular triangulation approximating  $\Sigma$ , with  $h^\Sigma$  the maximum element diameter. Let  $N^\Sigma$  denote the number of nodes in  $\mathcal{S}_h$  and let  $\mathcal{N}^\Sigma := \{1, \dots, N^\Sigma\}$  be the corresponding index set.

The averaged fracture pressure is discretized using first-order Lagrangian finite elements on  $\Sigma$ . We denote this finite element space by

$$V_{F,h}^\Sigma = \text{span}\{\varphi_i^\Sigma\}_{i \in \mathcal{N}^\Sigma},$$

with nodal basis functions  $\varphi_i^\Sigma : \Sigma \rightarrow \mathbb{R}$  associated with the fracture grid nodes  $\mathbf{s}_i$ ,  $i \in \mathcal{N}^\Sigma$ . For a function  $p_h^\Sigma \in V_{F,h}^\Sigma$  we denote by  $p_i^\Sigma$  its coefficient with respect to  $\varphi_i^\Sigma$  for all  $i \in \mathcal{N}^\Sigma$ .

### 5.2 XFEM Spaces for the Bulk Problems

We assume that  $\tilde{\Omega}$  is a polygon and denote by  $\mathcal{T}_h$  a conforming and shape regular triangulation of  $\tilde{\Omega}$ . Let  $h^\Omega$  denote the maximal diameter of an element of  $\mathcal{T}_h$ , and  $N^\Omega$  the number of nodes in  $\mathcal{T}_h$ . The corresponding index set is  $\mathcal{N}^\Omega := \{1, \dots, N^\Omega\}$ .

For a fixed  $R \geq 0$ , denote by  $\mathcal{J}_R$  the set of indices of nodes that are within a cylindrical region around the crack front with radius  $R$ , or are contained in elements that intersect the crack front

$$\mathcal{J}_R := \{i \in \mathcal{N}^\Omega \mid \exists T \in \mathcal{T}_h \text{ with } \mathbf{x}_i \in T \text{ and } \gamma \cap T \neq \emptyset \text{ or } \text{dist}(\mathbf{x}_i, \partial\Sigma) \leq R\}.$$

Further, introduce the set of indices of nodes contained in elements that are cut by the crack, but not already contained in  $\mathcal{J}_R$ ,

$$\mathcal{K}_R := \{i \in \mathcal{N}^\Omega \setminus \mathcal{J}_R \mid \exists T \in \mathcal{T}_h \text{ with } \Sigma \cap T \neq \emptyset\}.$$

Furthermore we introduce the standard finite element function  $\varphi_i^\Omega : \tilde{\Omega} \rightarrow \mathbb{R}$  associated with the bulk grid node  $i$ , and the Heaviside function  $H : \tilde{\Omega} \rightarrow \mathbb{R}$ ,

$$H(\mathbf{x}) = \begin{cases} -1 & \text{if } \mathbf{x} \in \Omega^-, \\ 1 & \text{else.} \end{cases} \quad (24)$$

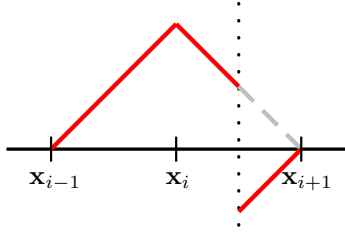


Figure 3: 1D Heaviside shape function  $H\varphi_i^\Omega$

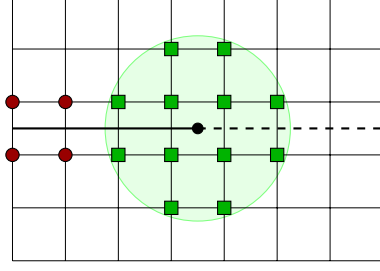


Figure 4: Node types for 2D enrichment – red circles: Heaviside enriched nodes; green squares: crack tip function enriched nodes

### 5.2.1 Discrete Displacement Space

We define  $\mathbf{e}_\alpha$  as the  $\alpha$ -th canonical basis vector of  $\mathbb{R}^d$ , and

$$\mathbf{V}_{E,h} := \text{span} \left[ \bigcup_{\alpha=1}^d \left( \{\varphi_i^\Omega \mathbf{e}_\alpha\}_{i \in \mathcal{N}^\Omega} \cup \{H\varphi_i^\Omega \mathbf{e}_\alpha\}_{i \in \mathcal{K}_R} \cup \{F_j \varphi_i^\Omega \mathbf{e}_\alpha \mid j \in \{1, 2, 3, 4\}, i \in \mathcal{J}_R\} \right) \right],$$

and

$$\{F_j(r, \Theta)\}_{j=1}^4 = \left\{ \sqrt{r} \sin\left(\frac{\Theta}{2}\right), \sqrt{r} \cos\left(\frac{\Theta}{2}\right), \sqrt{r} \sin\left(\frac{\Theta}{2}\right) \sin(\Theta), \sqrt{r} \cos\left(\frac{\Theta}{2}\right) \sin(\Theta) \right\}. \quad (25)$$

Here  $(r, \Theta)$  are the polar coordinates around the crack front introduced in Section 4.1.1.

The tip enrichment functions  $F_j$ ,  $j = 1, \dots, 4$ , are the standard enrichment functions in the XFEM theory for linear elasticity problems. As shown in Theorem 19 these functions span the first order asymptotic expansion in a neighborhood of the crack tip.

We can represent each function  $\mathbf{u}_h = \sum_{\alpha=1}^d u_{h,\alpha}^\Omega \mathbf{e}_\alpha \in \mathbf{V}_{E,h}$  by

$$u_{h,\alpha}^\Omega(\mathbf{x}) = \sum_{i \in \mathcal{N}^\Omega} u_{i,\alpha} \varphi_i^\Omega(\mathbf{x}) + \sum_{i \in \mathcal{J}_R} v_{i,\alpha} H(\mathbf{x}) \varphi_i^\Omega(\mathbf{x}) + \sum_{i \in \mathcal{K}_R} \sum_{j=1}^4 c_{i,\alpha}^{(j)} F_j(\mathbf{x}) \varphi_i^\Omega(\mathbf{x}), \quad \alpha = 1, \dots, d.$$

The average and jump of  $\mathbf{u}_h$  at the fracture can be determined easily using only coefficient values and the standard Lagrangian hat function

$$\begin{aligned} \llbracket u_{h,\alpha}^\Omega(\mathbf{s}) \rrbracket &= \sum_{i \in \mathcal{J}_R} 2v_{i,\alpha} \varphi_i^\Omega(\mathbf{s}) + \sum_{i \in \mathcal{K}_R} 2c_{i,\alpha}^{(1)} \sqrt{r(\mathbf{s})} \varphi_i^\Omega(\mathbf{s}), \\ \{u_{h,\alpha}^\Omega(\mathbf{s})\} &= \sum_{i \in \mathcal{N}^\Omega} u_{i,\alpha} \varphi_i^\Omega(\mathbf{s}), \end{aligned}$$

for all  $\mathbf{s} \in \Sigma$ . These relations make this set of enrichment functions particularly easy to work with.

### 5.2.2 Discrete Pressure Space

The discretization space of the bulk pore pressure is defined by

$$V_{F,h}^\Omega := \text{span}\{\varphi_i^\Omega\}_{i \in \mathcal{N}^\Omega} \cup \text{span}\{H\varphi_i^\Omega\}_{i \in \mathcal{K}_R} \cup \text{span}\{G_j \varphi_i^\Omega \mid j = 1, 2\}_{i \in \mathcal{J}_R},$$

where  $H$  is Heaviside function (24) and

$$G_1(r, \Theta) = F_1(r, \Theta) = \sqrt{r} \sin\left(\frac{\Theta}{2}\right), \quad G_2(r, \Theta) = F_2(r, \Theta) = \sqrt{r} \cos\left(\frac{\Theta}{2}\right). \quad (26)$$

As mentioned in Remark 21, the functions  $G_1$  and  $G_2$  span the first order asymptotic expansion in the near-tip approximation of the solution of the Laplace equation. Each  $p_h^\Omega \in V_{F,h}^\Omega$  can be represented by

$$p_h^\Omega(\mathbf{x}) = \sum_{i \in \mathcal{N}^\Omega} p_i^\Omega \varphi_i^\Omega(\mathbf{x}) + \sum_{i \in K_r} q_i^\Omega H(\mathbf{x}) \varphi_i^\Omega(\mathbf{x}) + \sum_{i \in J_r} \sum_{j=1}^2 r_{ij}^\Omega G_j(r, \Theta) \varphi_i^\Omega(\mathbf{x}).$$

As for the displacement enrichment functions, we have for all  $\mathbf{s} \in \Sigma$  that

$$\begin{aligned} \llbracket p_h^\Omega(\mathbf{s}) \rrbracket &= \sum_{i \in J_r} 2q_i^\Omega \varphi_i^\Omega(\mathbf{s}) + \sum_{i \in K_r} 2r_{i1}^\Omega \sqrt{r} \varphi_i^\Omega(\mathbf{s}), \\ \{p_h^\Omega(\mathbf{s})\} &= \sum_{i \in \mathcal{N}^\Omega} p_i^\Omega \varphi_i^\Omega(\mathbf{s}). \end{aligned}$$

Hence the average and the jump of a pressure finite element function can be easily evaluated.

### 5.3 Discrete Coupled Problems

The finite element spaces defined in the previous sections are conforming, and we can therefore obtain the discrete problem formulation by restricting the weak problem (22) to the finite element spaces. The result reads: Find  $(\mathbf{u}_h, p_h^\Omega, p_h^\Sigma) \in \mathbf{V}_{E,h} \times V_{F,h}^\Omega \times V_{F,h}^\Sigma$  such that

$$a_F^\Omega(\mathbf{u}_h, p_h^\Omega, r_h^\Omega) - c_F(\mathbf{u}_h, p_h^\Sigma, r_h^\Omega) = l_F^\Omega(r_h^\Omega) \quad \forall r_h^\Omega \in V_{F,h}^\Omega, \quad (27a)$$

$$a_F^\Sigma(\mathbf{u}_h, p_h^\Sigma, r_h^\Sigma) - c_F(\mathbf{u}_h, r_h^\Sigma, p_h^\Omega) = l_F^\Sigma(\mathbf{u}_h, r_h^\Sigma) \quad \forall r_h^\Sigma \in V_{F,h}^\Sigma, \quad (27b)$$

$$a_E(\mathbf{u}_h, \mathbf{v}_h) - c_E^\Omega(\mathbf{v}_h, p_h^\Omega) + c_E^\Sigma(\mathbf{v}_h, p_h^\Sigma) = l_E^\Omega(\mathbf{v}_h) \quad \forall \mathbf{v}_h \in \mathbf{V}_{E,h}. \quad (27c)$$

In view of numerically solving this system with a substructuring method, we write it as two separate linear problems, connected by a nonlinear coupling condition. The first subproblem is the discrete coupled fluid–fluid problem: For given  $b_h \in H_{00}^{\frac{1}{2}}(\Sigma)$ , find  $(p_h^\Omega, p_h^\Sigma) \in V_{F,h}^\Omega \times V_{F,h}^\Sigma$  such that

$$a_{F,b_h}^\Omega(p_h^\Omega, r_h^\Omega) - c_{F,b_h}(p_h^\Sigma, r_h^\Omega) = l_{F,b_h}^\Omega(r_h^\Omega) \quad \forall r_h^\Omega \in V_{F,h}^\Omega, \quad (28a)$$

$$a_{F,b_h}^\Sigma(p_h^\Sigma, r_h^\Sigma) - c_{F,b_h}(r_h^\Sigma, p_h^\Omega) - c_{F,\kappa,b_h}(r_h^\Sigma, p_h^\Omega) = l_{F,b_h}^\Sigma(r_h^\Sigma) \quad \forall r_h^\Sigma \in V_{F,h}^\Sigma. \quad (28b)$$

The second subproblem is the discrete weak elasticity problem: For given  $(p_h^\Omega, p_h^\Sigma) \in V_{F,h}^\Omega \times V_{F,h}^\Sigma$ , find  $\mathbf{u}_h \in \mathbf{V}_{E,h}$  such that

$$a_E(\mathbf{u}_h, \mathbf{v}_h) = l_{E,p_h^\Sigma,p_h^\Omega}(\mathbf{v}_h) \quad \forall \mathbf{v}_h \in \mathbf{V}_{E,h}. \quad (29)$$

The two subproblems are coupled nonlinearly via the discrete crack width function

$$b_h(\mathbf{s}) := \llbracket \mathbf{u}_h(\mathbf{s}) \rrbracket \cdot \nu = \sum_{\alpha=1}^d \left[ \sum_{i \in J_r} 2v_{i,\alpha} \varphi_i(\mathbf{s}) \nu_\alpha + \sum_{i \in K_r} 2c_{i,\alpha}^{(1)} \sqrt{r(\mathbf{s})} \varphi_i(\mathbf{s}) \nu_\alpha \right], \quad \mathbf{s} \in \Sigma.$$

The space of all discrete crack width functions is denoted by

$$H_h^{\frac{1}{2}} := \text{span}\{\varphi_i \nu_\alpha \mid i \in K_r, \alpha = 1, \dots, d\} \cup \text{span}\{\sqrt{r} \varphi_i \nu_\alpha \mid i \in J_r, \alpha = 1, \dots, d\}$$

and we remark that this is a subspace of  $H_{00}^{\frac{1}{2}}(\Sigma)$ .

Existence and uniqueness of solutions to the subproblems are direct consequences of Theorems 18 and 20.

In [27] the following optimal convergence result for the elasticity subproblem (29) was proved for two-dimensional domains.

**Theorem 22.** *Assume that the displacement solution  $\mathbf{u}$  of Problem (16) satisfies*

$$\mathbf{u} - \mathbf{u}_s \in H^2(\Omega),$$

where  $\mathbf{u}_s$  denotes the singular part of  $\mathbf{u}$  near the crack tip. Denote by  $\mathbf{u}_h$  the solution of problem (29) and let  $\chi$  be a smooth cutoff function at the crack tip. Then

$$\|\mathbf{u} - \mathbf{u}_h\|_{1,\Omega} \lesssim h \|\mathbf{u} - \chi \mathbf{u}_s\|_{2,\Omega}.$$

No corresponding result for the pressure subproblem is known.

## 5.4 Substructuring Solver

It is convenient to solve the nonlinear coupled problem (27) by iterating between the linear subproblems (28) and (29).

We suppose in the following that the discrete crack width function remains greater than zero away from the crack tip. Let  $k = 1, 2, \dots$  be the iteration number,  $b_{h,0} \in H_h^{\frac{1}{2}}$  be an initial discrete fracture width function, and  $\beta \in (0, 1]$  a damping parameter. The substructuring solver proceeds in four steps:

1. Solve the coupled fluid–fluid problem: Find  $(p_k^\Sigma, p_k^\Omega) \in V_{F,h}^\Sigma \times V_{F,h}^\Omega$  such that

$$\begin{aligned} a_{F,b_{k-1}}^\Omega(p_k^\Omega, r^\Omega) - c_{F,b_{k-1}}(p_k^\Sigma, r^\Omega) &= l_F^\Omega(r^\Omega) & \forall r^\Omega \in V_{F,h}^\Omega, \\ a_{F,b_{k-1}}^\Sigma(p_k^\Sigma, r^\Sigma) - c_{F,b_{k-1}}(r^\Sigma, p_k^\Omega) &= l_{F,b_{k-1}}^\Sigma(r^\Sigma) & \forall r^\Sigma \in V_{F,h}^\Sigma, \end{aligned}$$

2. Solve the elasticity problem: Find  $\tilde{\mathbf{u}}_k \in \mathbf{V}_{E,h}$  such that

$$a_{E,p_k^\Sigma,p_k^\Omega}^\Omega(\tilde{\mathbf{u}}_k, \mathbf{v}) = l_{E,p_k^\Sigma,p_k^\Omega}(\mathbf{v}) \quad \forall \mathbf{v} \in \mathbf{V}_{E,h},$$

3. Damped update:

$$\mathbf{u}_k := (1 - \beta) \mathbf{u}_{k-1} + \beta \tilde{\mathbf{u}}_k.$$

4. Compute the normal jump at the fracture:

$$b_k := \llbracket \mathbf{u}_k \rrbracket \cdot \nu.$$

A rigorous proof of convergence of this iteration is left for future work. In numerical experiments we observe a very fast convergence (Section 6.1).

## 6 Numerical Results

We close the article by giving a few numerical results. In particular, we show that the discretization error of the XFEM discretization proposed in the previous section behaves optimally when the mesh is refined. This justifies our choice of enrichment functions. Besides that, we show that the substructuring method converges very fast. Finally, we give a three-dimensional simulation. Our implementation is based on the DUNE libraries<sup>1</sup>, with the `dune-grid-glue`<sup>2</sup> module to couple the bulk and fracture grids [3]. To solve systems of linear equations we use the UMFPACK direct solver [8].

<sup>1</sup>[www.dune-project.org](http://www.dune-project.org)

<sup>2</sup>[www.dune-project.org/modules/dune-grid-glue](http://www.dune-project.org/modules/dune-grid-glue)

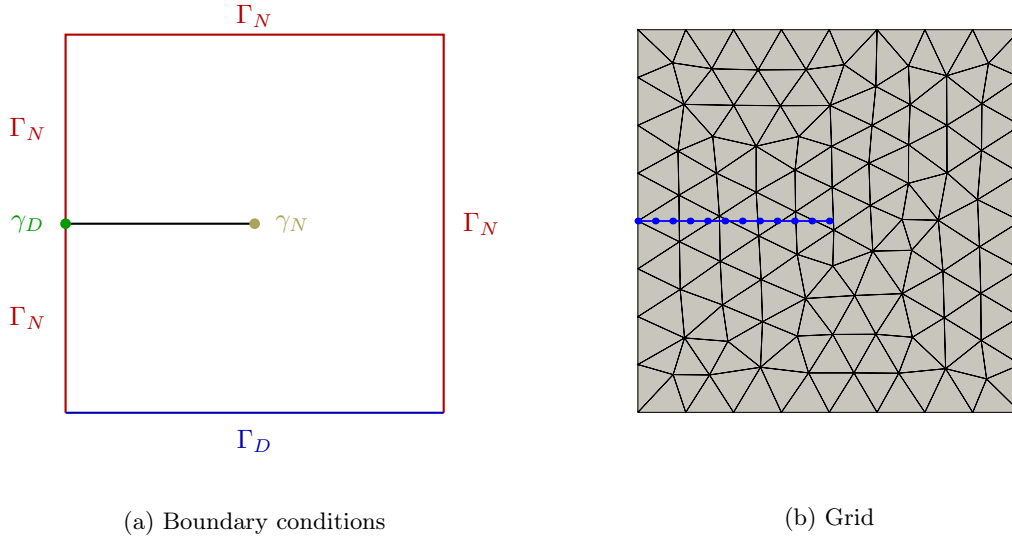


Figure 5: Problem setting

## 6.1 Substructuring Solver Convergence

To investigate the convergence rate of the iterative solver we consider a two-dimensional problem on the domain  $\Omega = [0, 1] \times [-\frac{1}{2}, \frac{1}{2}]$  (lengths are in kilometer). The midsurface of the fracture is given by  $\Sigma = [0, \frac{1}{2}] \times \{0\}$ . The permeability tensors in the bulk and in the fracture domains are homogeneous and isotropic, with  $K = 0.1 \text{ mD}$  for the bulk and  $K^\nu = K^\tau = 100 \text{ D}$  for the fracture. With these values the fluid can flow easily along and across the fracture, whereas the rock matrix is much less permeable. Mechanically, the solid skeleton behaves according to the St. Venant–Kirchhoff material law with Young’s modulus  $E = 1 \text{ GPa}$  and Poisson ratio  $\nu = 0.3$ .

We prescribe zero Dirichlet boundary conditions for both the fluid problem and the elasticity problem on the lower boundary of the bulk domain. Furthermore, a prescribed Dirichlet pressure of  $p_0^\Sigma = 0.5 \text{ MPa}$  is applied to the left boundary of the fracture  $\gamma_D$ . Zero Neumann boundary conditions are applied to the remaining parts of  $\partial\Omega$ , and to the crack tip  $\gamma_N$  (see Figure 5a). We set the XFEM enrichment radius to  $R = 0.125$ , the solver damping parameter  $\beta$  to one, and prescribe the initial crack width function  $b_{h,0} = \sqrt{r} \cdot 10^{-2} \text{ m}$ .

We discretize the bulk domain with an unstructured triangle grid, and the fracture domain with a uniform one-dimensional grid. Both grids are shown in Figure 5b. We create hierarchies of grids of different mesh size by refining both of them uniformly. For the test for the solver convergence speed we use up to 4 steps of uniform refinement.

To measure the solver speed for a given pair of bulk and fracture grids, we compute a reference solution  $(p_{h,*}^\Omega, p_{h,*}^\Sigma, \mathbf{u}_{h,*})$  by performing 20 substructuring iterations. After this many iterations, the solver is well beyond the limit of machine accuracy. We then compute the algebraic error of any iteration  $(p_{h,k}^\Omega, p_{h,k}^\Sigma, \mathbf{u}_{h,k})$ ,  $k = 1, 2, \dots$ , as the relative  $H^1$ -error against this reference solution

$$\text{err}_k = \frac{\|(p_{h,*}^\Omega, p_{h,*}^\Sigma, \mathbf{u}_{h,*}) - (p_{h,k}^\Omega, p_{h,k}^\Sigma, \mathbf{u}_{h,k})\|_1}{\|(p_{h,*}^\Omega, p_{h,*}^\Sigma, \mathbf{u}_{h,*})\|_1}.$$

The result of the test can be seen in Figure 6, where we have plotted the algebraic error as a function of the iteration number  $k$  for the different grid sizes. The error per iteration decays linearly on a logarithmic scale at a very fast rate. Indeed, a reduction of the relative error by a factor of  $10^{-8}$  is achieved within only 5 iteration steps, and the convergence rate appears to be almost completely independent of the mesh size. We conclude that the substructuring method is a very competitive way to solve the coupled bulk–fracture system.

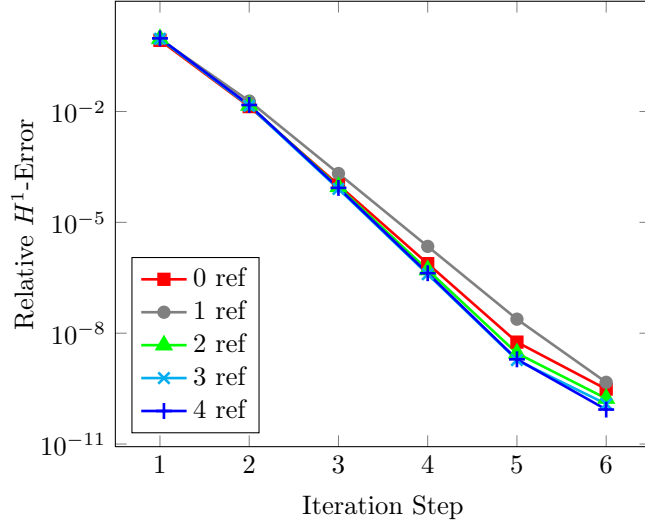


Figure 6: Solver convergence

## 6.2 Discretization Error Measurements

We now measure the discretization error of the XFEM discretization proposed in Section 5. This is a crucial experiment: The choice of the special tip enrichment functions (25) and (26) can only be justified if the resulting discretization error behaves optimally as a function of the mesh size.

We use the same benchmark problem as in the previous section. For each refinement level  $j$  we have computed reference solutions  $(p_{h,*}^{\Omega,j}, p_{h,*}^{\Sigma,j}, \mathbf{u}_{h,*}^j)$ , for which the algebraic error is below  $10^{-9}$ . Of these five triples of functions, we pick  $(p_{h,*}^{\Omega,4}, p_{h,*}^{\Sigma,4}, \mathbf{u}_{h,*}^4)$ , the one on the finest grid, to be the reference solution, and we compute  $L^2$  and  $H^1$  errors for the coarser four solutions. The results of this test can be seen in Figure 7. The errors are split up into the three components, that is: the matrix displacement  $\mathbf{u}$ , the bulk fluid pressure  $p^\Omega$ , and the fracture fluid pressure  $p^\Sigma$ . All three components show optimal error behavior, i.e., a decay of at least  $\mathcal{O}(h^2)$  for the  $L^2$  error and a decay of  $\mathcal{O}(h)$  for the  $H^1$  error. The discretization error of the bulk pressure  $p^\Omega$  behaves even better. The  $L^2$  error decays like  $\mathcal{O}(h^3)$  and the  $H^1$  error as  $\mathcal{O}(h^{\frac{3}{2}})$ . This may be due to the fact that for this particular example the matrix pressure is continuous over the fracture and that the singularity of the fluid pressure gradient at the crack tip is reproduced by the second enrichment function  $G_2$ . The  $L^2$  error of the fracture pressure behaves like  $\mathcal{O}(h^2)$ , which is better than expected as well. The reason for this is unclear. We conjecture that the higher regularity of the matrix pressure leads to a higher regularity in the coupling terms as well, and hence a stabilization effect for the fracture pressure gradient is induced.

## 6.3 A Three-Dimensional Example

Finally, we demonstrate that our approach and implementation also work for three-dimensional problems. We consider the domain  $\Omega = [0, 1] \times [-1/2, 1/2] \times [-1/2, 1/2]$ , again in kilometers. The midsurface of the fracture is defined as a half disc with radius  $R = \frac{1}{4}$  km and center  $(0, 0, 0)^T$ . The material properties are set as in the two-dimensional example, i.e., the bulk permeability is  $K = 0.1$  mD, the fracture permeabilities are  $K^\nu = K^\tau = 100$  D and for the matrix stiffness we set  $E = 1$  GPa and  $\nu = 0.3$ .

We apply zero Dirichlet boundary conditions on the bottom and zero Neumann boundary conditions on the remaining part of the cube for the fluid bulk pressure and the displacement. We prescribe a fracture pressure  $p_0^\Sigma = 0.5$  MPa at the boundary part  $\gamma_D = \{0\} \times [-1/4, 1/4] \times \{0\}$  and zero Neumann

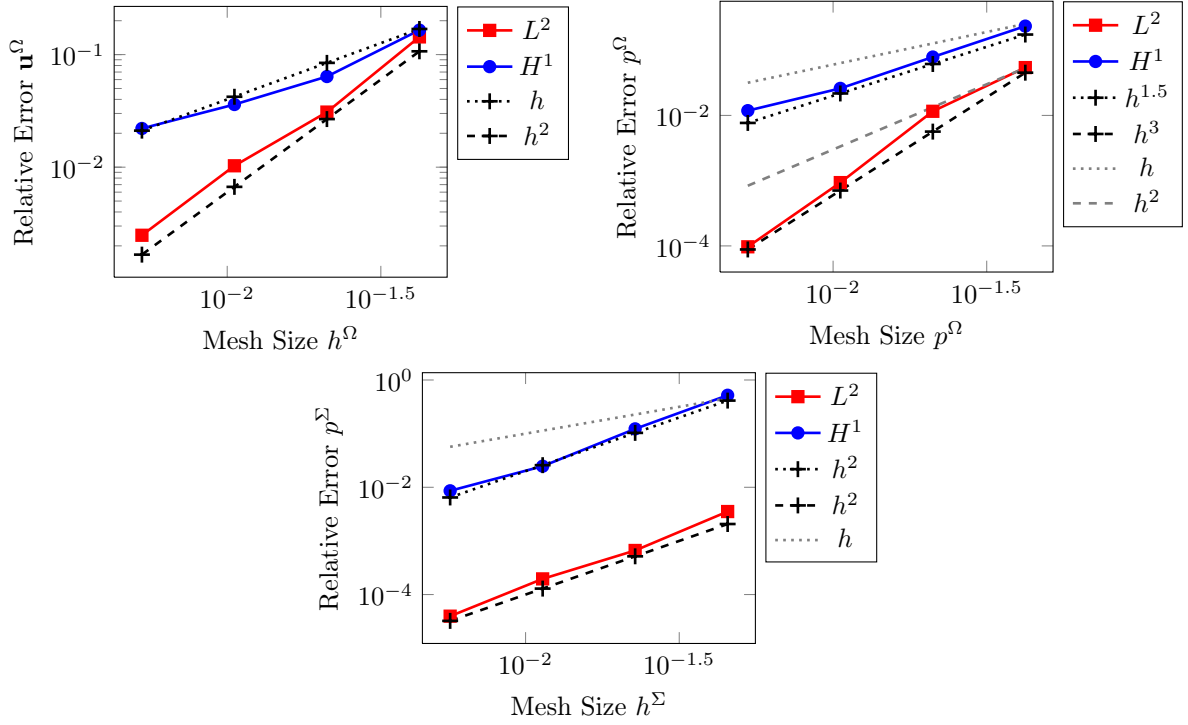


Figure 7: Discretization error

conditions everywhere else on the boundary of the midsurface (see Figure 8).

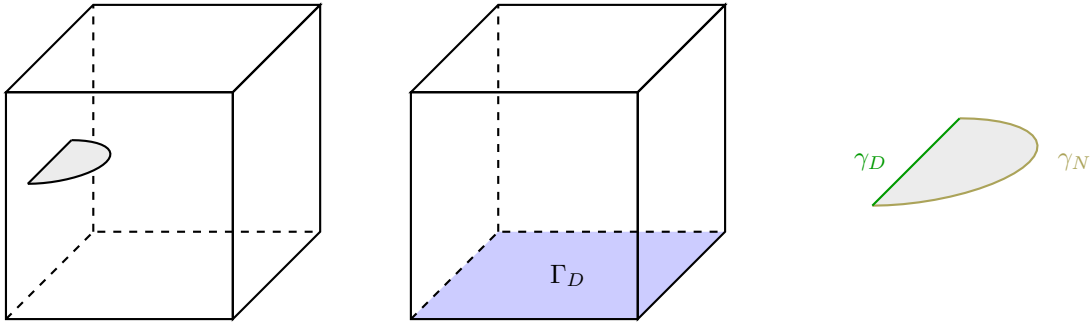


Figure 8: Boundary Conditions for the three-dimensional example

The bulk domain is discretized using a structured tetrahedral grid with 20250 elements in total. The interface grid is an unstructured triangle grid with 90 elements. The XFEM enrichment radius is set to  $R = 0.125$ ,  $\beta$  to one, and the initial crack width function is set to  $b_{h,0} = \sqrt{r} \cdot 10^{-2}$  m. We compute the von Mises stress of the displacement by evaluating the stress in the center of the elements. Nodal values are computed by averaging the values of the elements the node is contained in. The result of this computation can be seen in Figure 9.

For this example, the substructuring solver again converges in very few iterations. In the outcome, we observe that the fracture pressure is nearly constant. The fluid flows out of the fracture and thus

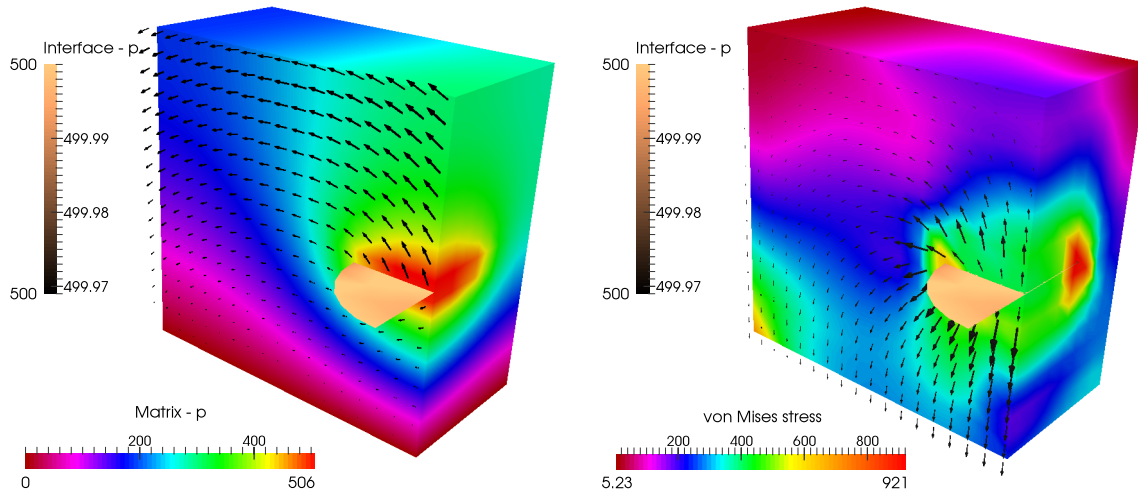


Figure 9: Results of the three-dimensional example; Left: Bulk pressure, displacement (scaled by 100) and interface pressure; Right: Von Mises stress of the displacement field, bulk flow (scaled by  $5 \cdot 10^3$ ) and interface pressure.

a force is applied onto the fracture boundaries inducing a deformation, which opens the fracture. The von Mises stress induced by the deformation has a maximum at the fracture front, which would lead to an enlargement of the fracture if fracture growth was included in the model.

## References

- [1] M.H. Aliabadi. Boundary element formulations in fracture mechanics. *Applied Mechanics Reviews*, 50:83–96, 1997.
- [2] P. Angot, F. Boyer, and F. Hubert. Asymptotic and numerical modelling of flows in fractured porous media. *ESAIM: Mathematical Modelling and Numerical Analysis*, 43:239–275, 2009.
- [3] P. Bastian, M. Blatt, A. Dedner, C. Engwer, R. Klöfkorn, R. Kornhuber, M. Ohlberger, and O. Sander. A generic grid interface for parallel and adaptive scientific computing. part ii: implementation and tests in dune. *Computing*, 82(2-3):121–138, 2008.
- [4] B. Bourdin, G.A. Francfort, and J.-J. Marigo. The variational approach to fracture. *Journal of Elasticity*, 91(1-3):5–148, 2008.
- [5] Kevin Brewster and Marius Mitrea. In weighted sobolev spaces on lipschitz manifolds. *Memoirs on Differential Equations and Mathematical Physics*, 60:15–55, 2013.
- [6] M. Costabel and M. Dauge. General edge asymptotics of solutions of second-order elliptic boundary value problems i. *Proceedings of the Royal Society of Edinburgh: Section A Mathematics*, 123(01):109–155, 1993.
- [7] C. D’Angelo and A. Scotti. A mixed finite element method for darcy flow in fractured porous media with non-matching grids. *ESAIM: Mathematical Modelling and Numerical Analysis*, 46:465–489, 2012.
- [8] T. Davis. Suitesparse project homepage. URL: <http://faculty.cse.tamu.edu/davis/welcome> (visited on 05/03/2015)

- [9] R. G. Durán and F. López García. Solutions of the divergence and analysis of the stokes equations in planar hölder- $\alpha$  domains. *Mathematical Models and Methods in Applied Sciences*, 20(01):95–120, 2010.
- [10] D. E. Edmunds and B. Opic. Weighted poincaré and friedrichs inequalities. *Journal of the London Mathematical Society*, s2-47(1):79–96, 1993.
- [11] L. Formaggia, A. Fumagalli, A. Scotti, and P. Ruffo. A reduced model for darcy’s problem in networks of fractures. *ESAIM: Mathematical Modelling and Numerical Analysis*, 48:1089–1116, 2014.
- [12] T.-P. Fries, M. Schätzer, and N. Weber. XFEM-Simulation of Hydraulic Fracturing in 3D with Emphasis on Stress Intensity Factors. In: *11th World Congress on Computational Mechanics (WCCM XI) and 5th European Congress on Computational Mechanics (ECCM V) and 6th European Congress on Computational Fluid Dynamics (ECFD VI)*. (Barcelona, Spain). Ed. by E. Oñate, X. Oliver, and A. Huerta, CIMNE, pages 3282–3293, 2014.
- [13] A. Fumagalli and A. Scotti. A numerical method for two-phase flow in fractured porous media with non-matching grids. *Advances in Water Resources*, 62, Part C:454 – 464, 2013. Computational Methods in Geologic CO2 Sequestration.
- [14] A. Fumagalli and A. Scotti. A reduced model for flow and transport in fractured porous media with non-matching grids. In A. Cangiani, R.L. Davidchack, E. Georgoulis, A.N. Gorban, J. Levesley, and M.V. Tretyakov, editors, *Numerical Mathematics and Advanced Applications 2011*, pages 499–507. Springer, 2013.
- [15] D.I. Garagash, E. Detournay, and J.I. Adachi. Multiscale tip asymptotics in hydraulic fracture with leak-off. *Journal of Fluid Mechanics*, 669:260–297, 2011.
- [16] V. Girault, K. Kumar, and M. F. Wheeler. Convergence of iterative coupling of geomechanics with flow in a fractured poroelastic medium. *Computational Geosciences*, 2016.
- [17] V. Girault, M. F. Wheeler, B. Ganis, and M. E. Mear. A lubrication fracture model in a poro-elastic medium. *Mathematical Models and Methods in Applied Sciences*, 25(04):587–645, 2015.
- [18] C.E. Inglis. Stresses in plates due to the presence of cracks and sharp corners. *Transactions of the Institute of Naval Architects*, 55:219–241, 1913.
- [19] J. Jaffré, M. Mnejja, and J.E. Roberts. A discrete fracture model for two-phase flow with matrix-fracture interaction. *Procedia Computer Science*, 4(0):967–973, 2011. Proceedings of the International Conference on Computational Science, {ICCS} 2011.
- [20] A.M. Khludnev and V.A. Kovtunenکو. *Analysis of Cracks in Solids*. International series on advances in fracture. WIT Press, 2000.
- [21] V. Kozlov, V.G. Mazia, and J. Rossmann. *Spectral Problems Associated with Corner Singularities of Solutions to Elliptic Equations*. Mathematical surveys and monographs. American Mathematical Society, 2001.
- [22] A. Kufner and B. Opic. How to define reasonably weighted sobolev spaces. *Commentationes Mathematicae Universitatis Carolinae*, 025(3):537–554, 1984.
- [23] Vincent Martin, Jérôme Jaffré, and Jean E. Roberts. Modeling fractures and barriers as interfaces for flow in porous media. *SIAM Journal on Scientific Computing*, 26(5):1667–1691, 2005.
- [24] A. Mikelić, M. F. Wheeler, and T. Wick. A Phase-Field Method for Propagating Fluid-Filled Fractures Coupled to a Surrounding Porous Medium. *Multiscale Modeling & Simulation*, 13(1):367–398, 2015.

- [25] N. Miller. Weighted sobolev spaces and pseudodifferential operators with smooth symbols. *Transactions of the American Mathematical Society*, 269(1):91–109, 1982.
- [26] N. Moës, J. Dolbow, and T. Belytschko. A finite element method for crack growth without remeshing. *International Journal for Numerical Methods in Engineering*, 46(1):131–150, 1999.
- [27] Serge Nicaise, Yves Renard, and Elie Chahine. Optimal convergence analysis for the extended finite element method. *International Journal for Numerical Methods in Engineering*, 86(4-5):528–548, 2011.
- [28] B. Opic and A. Kufner. *Hardy-type Inequalities*. Pitman research notes in mathematics series. Longman Scientific & Technical, 1990.
- [29] S. Pommier, A. Gravouil, N. Moës, and A. Combescure. *Extended Finite Element Method for Crack Propagation*. Iste Series. Wiley, 2011.
- [30] Alfio Quarteroni and Alberto Valli. *Domain Decomposition Methods for Partial Differential Equations*. Oxford Science Publications, 1999.
- [31] T. Rabczuk, S. Bordas, and G. Zi. Computational methods for fracture. *Mathematical Problems in Engineering*, 2014, 2014.
- [32] J. R. Rice. Mathematical analysis in the mechanics of fracture. *Fracture: an advanced treatise*, 2:191–311, 1968.
- [33] B.O. Turesson. *Nonlinear Potential Theory and Weighted Sobolev Spaces*. Number Nr. 1736 in Lecture Notes in Mathematics. Springer, 2000.
- [34] N. Watanabe, W. Wang, J. Taron, U. J. Görke, and O. Kolditz. Lower-dimensional interface elements with local enrichment: application to coupled hydro-mechanical problems in discretely fractured porous media. *International Journal for Numerical Methods in Engineering*, 90(8):1010–1034, 2012.
- [35] M. Wheeler, T. Wick, and W. Wollner. An augmented-lagrangian method for the phase-field approach for pressurized fractures. *Computer Methods in Applied Mechanics and Engineering*, 271(0):69–85, 2014.
- [36] J. Wloka. *Partial Differential Equations*. Cambridge University Press, 1987.
- [37] A. Yazid, N. Abdelkader, and H. Abdelmadjid. A state-of-the-art review of the x-fem for computational fracture mechanics. *Applied Mathematical Modelling*, 33(12):4269–4282, 2009.